

Emission from the D1D5 CFT: Higher Twists

Steven G. Avery^{1,*} and Borun D. Chowdhury^{2,†}

¹*Department of Physics
The Ohio State University
191 West Woodruff Avenue
Columbus, Ohio 43210-1117
U.S.A.*

²*Department of Theoretical Physics
Tata Institute of Fundamental Research
Homi Bhabha Road
Mumbai 400005
India*

Abstract

We study a certain class of nonextremal D1D5 geometries and their ergoregion emission. Using a detailed CFT computation and the formalism developed in [1], we compute the full spectrum and rate of emission from the geometries and find exact agreement with the gravity answer. Previously, only part of the spectrum had been reproduced using a CFT description. We close with a discussion of the context and significance of the calculation.

*Electronic address: avery@mps.ohio-state.edu

†Electronic address: borundev@mps.ohio-state.edu

1. INTRODUCTION

The background geometry created by certain stacks of branes can be broken into different regions. At asymptotic infinity, the geometry is flat. As one moves radially inward one comes into a “neck” region, which transitions between the flat space and an AdS “throat”. The AdS throat terminates in a “fuzzball” cap [2, 3, 4, 5, 6, 7, 8, 9, 10, 11, 12, 13, 14, 15, 16, 17, 18, 19, 20, 21, 22, 23, 24, 25, 26, 27, 28, 29, 30, 31, 32]; there are a large number of different caps with different structure. These geometries with different caps are interpreted as the microstates of the black hole formed from the branes. In general one expects the microstates to be quite quantum; however, in many cases one can find sets of classical supergravity solutions with different caps, which can be used to gain intuition about the structure of these microstates.

In [1], a general formalism was developed to compute the emission rate from the AdS region out into the asymptotically flat region using the AdS/CFT correspondence. In the low energy limit, modes living in the AdS region decouple from modes in the asymptotically flat region, and the physics of the AdS region is *dual* to the physics of an appropriate CFT [33, 34, 35]. One can consider, however, relaxing the strict decoupling limit and allowing some small amount of interaction between the AdS region and the flat region. Using the CFT description of the AdS physics, the interaction is described by adding a new term to the previously independent CFT and flat space actions, which couples flat space fields to vertex operators of the CFT. The formalism was demonstrated by computing the emission of minimal scalars from a subset of D1D5 states found in [2] and found exact agreement with the gravity calculation.

In this paper, we extend the results of [1] by computing the emission from a broader class of D1D5 states. In [36], the supergravity spectrum and rate of emission from this class of D1D5 geometries was *partially* reproduced by doing a heuristic CFT calculation. Our goal is to compute the rate of emission and *full* spectrum as a rigorous CFT calculation. This calculation serves to demonstrate the method of [1] in a more nontrivial calculation, and to tie up the loose ends of [36].

The D1D5 system we work with lives in a ten-dimensional geometry compactified on $T^4 \times S^1$. We wrap N_5 D5 branes on the full compact space, $T^4 \times S^1$; and we wrap N_1 D1 branes on the circle, S^1 . This gives rise to an $AdS_3 \times S^3$ throat in the noncompact space, which is dual to a two-dimensional CFT [37, 38, 39, 40, 41, 42, 43, 44, 45]. The core AdS region has radius $(Q_1 Q_5)^{\frac{1}{4}}$, where the D1 and D5 charges Q_1 and Q_5 are given by

$$Q_1 = \frac{g\alpha'^3}{V} N_1 \quad Q_5 = g\alpha' N_5, \quad (1.1)$$

with string coupling g and T^4 volume $(2\pi)^4 V$.

In [1], the emission rate of minimal scalars from this CFT_2 was found to be

$$\frac{d\Gamma}{dE} = \frac{2\pi}{2^{2l+1} l!^2} \frac{(Q_1 Q_5)^{l+1}}{R^{2l+3}} (E^2 - \lambda^2)^{l+1} |\langle 0 | \hat{\mathcal{V}}(0) | 1 \rangle_{\text{unit}}|^2 \delta_{\lambda, \lambda_0} \delta(E - E_0). \quad (1.2)$$

In the above equation, $2\pi R$ is the coordinate volume of the S^1 ; l is the angular momentum quantum number of the emitted minimal scalar; E and λ are the energy and momentum of the scalar along the S^1 ; and \mathcal{V} is the normalized vertex operator in the CFT that couples to the minimal scalar. The CFT amplitude is computed with “unit” S^1 coordinate $\sigma \in (0, 2\pi)$ and dimensionless Euclidean time $\tau = it/R$. The (σ, τ) dependence of the CFT amplitude has been integrated to give the energy-momentum conserving delta-functions, and then removed from the above equation by placing the vertex operator at the “origin”. The CFT states $|1\rangle$ and $|0\rangle$ are respectively the initial excited state and the final state of the CFT. They are dual to the initial and final states of the geometry’s capped AdS region.

The vertex operator for emission of supergravity minimal scalars is given by [1]

$$\tilde{\mathcal{V}}_{l,l-k-\bar{k},k-\bar{k}}^{A\dot{A}B\dot{B}}(\sigma, \tau) = \frac{1}{2} \sqrt{\frac{(l-k)!(l-\bar{k})!}{(l+1)^2(l+1)!^2 k! \bar{k}!}} (J_0^+)^k (\bar{J}_0^+)^{\bar{k}} G_{-\frac{1}{2}}^{+A} \psi_{-\frac{1}{2}}^{-\dot{A}} \bar{G}_{-\frac{1}{2}}^{+B} \bar{\psi}_{-\frac{1}{2}}^{-\dot{B}} \tilde{\sigma}_{l+1}^0(\sigma, \tau). \quad (1.3)$$

The subscript on $\tilde{\mathcal{V}}_{l,m_\psi,m_\phi}$ is its charge under the $SO(4)_E$ rotational symmetry of the S^3 . The numerical prefactor normalizes the operator so that it has unit two-point function with itself at unit separation in the complex plane. Mapping to the complex plane via

$$z = e^{\tau+i\sigma} \quad \bar{z} = e^{\tau-i\sigma}, \quad (1.4)$$

the vertex operator becomes

$$\begin{aligned} \tilde{\mathcal{V}}_{l,l-k-\bar{k},k-\bar{k}}^{A\dot{A}B\dot{B}}(\sigma, \tau) &= |z|^{l+2} \mathcal{V}_{l,l-k-\bar{k},k-\bar{k}}^{A\dot{A}B\dot{B}}(z, \bar{z}) \\ &= |z|^{l+2} \frac{1}{2} \sqrt{\frac{(l-k)!(l-\bar{k})!}{(l+1)^2(l+1)!^2 k! \bar{k}!}} (J_0^+)^k (\bar{J}_0^+)^{\bar{k}} G_{-\frac{1}{2}}^{+A} \psi_{-\frac{1}{2}}^{-\dot{A}} \bar{G}_{-\frac{1}{2}}^{+B} \bar{\psi}_{-\frac{1}{2}}^{-\dot{B}} \tilde{\sigma}_{l+1}^0(z, \bar{z}). \end{aligned} \quad (1.5)$$

For more details of the CFT notation, consult the appendix A of [1].

The remainder of the paper may be broken into the following steps:

1. In Section 2, we set up the physical emission problem from the geometries of [2], in the CFT language developed in [1]. Specifically, we describe the initial excited state and the final state that go into the CFT amplitude, which when plugged into Equation (1.2) give the emission rate of the minimal scalars. Evaluating the CFT amplitude is a nontrivial exercise, to which the majority of the paper is dedicated. The initial state is parameterized by three integers n , \bar{n} , and κ . The positive integer κ , called k in [36], controls a conical defect in the AdS region. The spectrum and rate of emission found in [1] were for $\kappa = 1$. In this paper, we extend those calculations to $\kappa > 1$.
2. We do not directly compute the physical CFT amplitude of interest. Instead, we compute a CFT amplitude that does *not* correspond to a physical gravitational process, and then map this “unphysical” amplitude onto the physical problem using spectral flow and hermitian conjugation. This route avoids some subtleties and allows us to use some results from [1] in the calculation. In Section 3, we precisely set up the unphysical CFT amplitude to be computed.
3. In Section 4, we show how to relate the unphysical amplitude to be computed to the physical problem using spectral flow and Hermitian conjugation.
4. Before starting the lengthy calculation of the unphysical CFT amplitude, in Section 5 we explain the specific method used to compute it. The unphysical amplitude, we explain, can be lifted to a covering space, where it becomes an amplitude computed in [1]. The Jacobian factors that arise in mapping to the covering space, however, are highly nontrivial. Additionally there are some important combinatoric factors, which come in from symmetrizing over all $N_1 N_5$ copies of the CFT.
5. In Section 6, we compute the Jacobian factors that arise from mapping the twist operators to the covering space. We use the methods for evaluating correlation functions of twist operators developed in [46].

6. In Section 7, we compute the Jacobian factors produced by the non-twist operator insertions in the unphysical amplitude.
7. In Section 9, we compute the combinatoric factors that come from symmetrizing over all $N_1 N_5$ copies of the CFT. The result simplifies in the large $N_1 N_5$ limit that is physically relevant.
8. Finally in Section 10, we use Section 4 to relate the computed unphysical amplitude to the final amplitude for emission. We then plug the amplitude into Equation (1.2) to find the rate of emission. The explicit κ -dependence comes in the form of a power, κ^{-2l-3} , multiplying the rate for $\kappa = 1$; the spectrum is also affected. The spectrum and rate exactly match the gravity calculation in [36].

Because this paper largely is a direct extension of [1], we do not introduce the notation used here in detail and instead refer the reader to Appendix A of [1] for an overview of the CFT notation. Furthermore, we take several results directly from [1].

2. EMISSION FROM κ -ORBIFOLDED GEOMETRIES

For a fixed amount of D1 charge, D5 charge, and S^1 -momentum, [2] found a three-parameter family of geometries that have the following properties. At infinity they are asymptotically flat, then as one goes radially inward one encounters a “neck” region. After passing through the neck, one finds an AdS throat which terminates in an ergoregion cap. The fuzzball proposal interprets these smooth, horizonless geometries as classical approximations to microstates of a black hole with the same charges.

The presence of ergoregions renders these geometries unstable [36, 47, 48]. The instability is exhibited by emission of particles at infinity, with exponentially increasing flux, carrying energy and angular momentum out of the geometry. In [36, 48, 49], using heuristic CFT computations for some special cases, it was argued that the ergoregion emission is the Hawking radiation from this subset of microstates for the D1D5 black hole. Figure 1 depicts the emission process in the gravity and CFT descriptions.

These geometries are dual to CFT states parameterized by three integers n , \bar{n} , and κ . In [1], the spectrum and rate of emission from the geometries with $\kappa = 1$ was exactly reproduced with a CFT computation. In this paper, we calculate the spectrum and rate of emission for $\kappa > 1$. The parameter κ (called k in [36]), controls a conical defect in the geometry. For $\kappa = 1$, there is no conical defect or orbifold singularity.

Below, we first describe the initial state of the physical CFT problem, which is dual to the unperturbed background geometry. Then, we roughly describe the final state of the physical CFT amplitude that the initial state decays to. We do not precisely give these states since we do not directly compute with them. In Section 3, we give the precise states used in the “unphysical” CFT amplitude, which in Section 4 we relate to the physically relevant states of this section.

2.1. The CFT initial state

The physical initial state is the background geometry described in [2] and [36]. The decoupled AdS-part of the geometry can be obtained by spectral flowing κ -orbifolded $AdS_3 \times S^3$ by $\alpha = 2n + \frac{1}{\kappa}$ units on the left-moving sector and by $\bar{\alpha} = 2\bar{n} + \frac{1}{\kappa}$ units on the right-moving sector. The fractional spectral flow may seem strange; however, it arises because of the conical defect. In [9, 50, 51] geometries were constructed which had a decoupled AdS part which can be understood

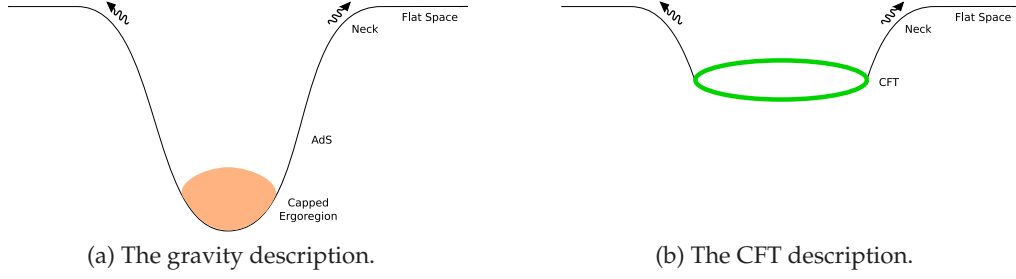


FIG. 1: A depiction of the emission process we consider. In the cap region of the geometry, there is an ergoregion (shown in orange), which leads to the emission of particles into the flat space. In the CFT description particles are emitted by the CFT (shown in green) directly into the “neck” region of the geometry.

in this context as spectral flow by $\alpha = 2n + \frac{1}{\kappa}$ and $\bar{\alpha} = \frac{1}{\kappa}$. However these geometries are BPS and do not have an ergoregion and thus do not radiate. We discuss fractional spectral flow in the CFT context in Section 4.1.

The κ -orbifolded AdS_3 is described, after a left and right spectral flow by $\frac{1}{\kappa}$, as twisting the $N_1 N_5$ strands into κ -length component strings in the R sector. This geometry is stable and does not emit anything. Performing further spectral flow, however, adds fermionic excitations to all of the component strings and allows for the possibility of emission.

The κ -twisted component string in the Ramond vacuum has weight $\kappa/4$. The Ramond vacuum also has “base spin” coming from the fermion zero modes. Let us start with the “spin up” κ -twisted Ramond vacuum with weight and charge

$$h = \bar{h} = \frac{\kappa}{4} \quad m = \bar{m} = \frac{1}{2}. \quad (2.1)$$

We then add energy and charge to this state by spectral-flowing by $2n$ units, where spectral flow by α units affects the weight and charge of a state by [52]

$$\begin{aligned} h &\mapsto h + \alpha m + \frac{\alpha^2 c_{\text{tot.}}}{24} \\ m &\mapsto m + \frac{\alpha c_{\text{tot.}}}{12}. \end{aligned} \quad (2.2)$$

Spectral flowing the κ -twisted Ramond vacuum by $2n$ units corresponds to filling all fermion energy levels up to the “Fermi sea level” $n\kappa$. Keep in mind that there are two complex fermions which have spin up and spectral flow fills fermion levels with both fermions. This gives the initial state’s weight and charge [36]

$$h_i = \kappa \left(n^2 + \frac{n}{\kappa} + \frac{1}{4} \right) \quad m_i = n\kappa + \frac{1}{2} \quad (2.3)$$

and similarly for the right sector replacing n by \bar{n} . This state is depicted in Figure 2(a).

2.2. The CFT final state

In emitting a particle of angular momentum (l, m_ψ, m_ϕ) the initial state is acted on by the supergravity vertex operator $\mathcal{V}_{l, -m_\psi, -m_\phi}$ from Equation (1.3).

We consider the process where the $(l+1)$ -twist operator acts on $l+1$ distinct component strings of the background forming one long $\kappa(l+1)$ -twisted component string. The final state, then, is

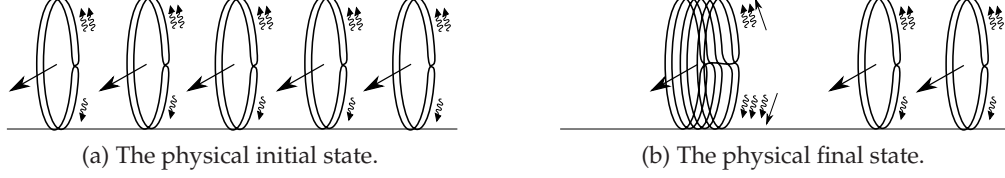


FIG. 2: A depiction of the initial and final states of the physical amplitude.

in the $\kappa(l+1)$ -twisted R sector. In principle there are other ways that the vertex operator may twist the initial state; however, we work in the limit where $N_1 N_5 \gg \kappa$, in which case this process dominates. Processes in which the vertex operator twists more than one strand of the same κ -length component string have probabilities suppressed by factors of $1/(N_1 N_5)$.

The charge/angular momentum of the vertex operator $\mathcal{V}_{l,l-k-\bar{k},k-\bar{k}}$ is given by

$$\begin{aligned} m_v &= -\left(\frac{l}{2} - k\right) & m_{\psi}^{\text{vertex}} &= -m_{\psi} = l - k - \bar{k} \\ \bar{m}_v &= -\left(\frac{l}{2} - \bar{k}\right) & m_{\phi}^{\text{vertex}} &= -m_{\phi} = k - \bar{k}. \end{aligned} \quad (2.4)$$

From the charge of the vertex operator and the initial state it is easy to deduce the charge of the final state:

$$m_f = (l+1)\left(n\kappa + \frac{1}{2}\right) - \left(\frac{l}{2} - k\right) = (l+1)n\kappa + k + \frac{1}{2}. \quad (2.5)$$

There can be different final states with the same charge corresponding to different harmonics of the emitted quanta. Since we derive the amplitude using spectral flowed states it is not important to write down the weights of the states here. However they are found easily by using the charge and weight of the spectral flowed states. The final state, which we call $|f\rangle$, is shown in Figure 2(b).

2.3. The physical CFT amplitude

From the initial and final states, the CFT amplitude which we use to find the emission spectrum and rate is given by

$$\mathcal{A}_{l,m_{\psi},m_{\phi}} = \langle f | \tilde{\mathcal{V}}_{l,m_{\psi},m_{\phi}}(\sigma, \tau) | i \rangle. \quad (2.6)$$

We prefer to calculate on the complex plane with z coordinates instead of on the cylinder. Mapping the vertex operator to the plane using Equation (1.4) gives a Jacobian factor, $|z|^{l+2}$, from its conformal weight. Thus, the physical CFT amplitude that we ultimately wish to find is written as

$$\mathcal{A}_{l,m_{\psi},m_{\phi}}(z) = |z|^{l+2} \langle f | \mathcal{V}_{l,m_{\psi},m_{\phi}}(z, \bar{z}) | i \rangle. \quad (2.7)$$

The majority of the paper is expended in calculating this amplitude. The tilde on the vertex operator in Equation (2.6) is to distinguish it from the operator in the complex plane.

3. THE “UNPHYSICAL” AMPLITUDE

We do not directly compute the amplitude of interest with the initial and final states described above. Instead we compute an amplitude, described below, that is related to the physical problem

by spectral flow and Hermitian conjugation. In this other amplitude, the calculation is simpler and we have a better understanding of what the initial and final states should be. In [1], the same technique was used.

In this section we describe the initial and final states of the unphysical amplitude, $|i'\rangle$ and $|f'\rangle$, that we use to calculate

$$\mathcal{A}' = \langle f' | \mathcal{V}(z) | i' \rangle. \quad (3.1)$$

Later, we relate this process to the physical problem by spectral flow and Hermitian conjugation. Before we can give the states, we must describe the notation we use, specifically addressing the fermions' periodicity.

3.1. Fermion periodicities

First, let us emphasize what the R and NS sectors *mean* in the twisted sector. We define two parameters β_+ and β_- , which specify the periodicity of the fermions in the theory:

$$\psi^{\pm\dot{A}}(ze^{2\pi i}) = e^{i\pi\beta_{\pm}} \psi^{\pm\dot{A}}(z). \quad (3.2)$$

Obviously, β_{\pm} are only defined modulo two under addition.

The R sector means $\beta_{\pm} \equiv 1$, whereas the NS sector means $\beta_{\pm} \equiv 0$. Spectral flow by α units has the effect of taking

$$\beta_{\pm} \mapsto \beta_{\pm} \pm \alpha. \quad (3.3)$$

In the p -twisted sector, the boundary conditions are

$$\psi_{(j)}^{\pm\dot{A}}(ze^{2\pi i}) = e^{i\pi\beta_{\pm}} \psi_{(j+1)}^{\pm\dot{A}}(z), \quad (3.4)$$

where (j) indexes the different copies of the target space. This implies that

$$\psi_{(j)}^{\pm\dot{A}}(ze^{2p\pi i}) = e^{ip\pi\beta_{\pm}} \psi_{(j)}^{\pm\dot{A}}(z). \quad (3.5)$$

In the base space, over each point z , there are p different copies of each field. To calculate, it is convenient to map to a covering space where these p copies become a single-valued field. When one goes to a covering space the periodicity of the total single-valued field $\Psi(t)$, then is given by

$$\Psi^{\pm\dot{A}}(te^{2\pi i}) = \exp[i(p\beta_{\pm} + (p-1))\pi] \Psi^{\pm\dot{A}}(t), \quad (3.6)$$

where the extra factor of $(p-1)$ in the exponent comes from the Jacobian of the weight-half fermion, under a map of the form $z \propto t^p$. We label the periodicity in the cover by

$$\beta_{\pm}^{(\text{cover})} = p(\beta_{\pm} + 1) - 1. \quad (3.7)$$

In the untwisted sector, we use the natural definition of the fermions, $\psi(z)$, as being periodic, without branch cut. Thus, application of a spin field operator is necessary to give antiperiodic boundary conditions. In the twisted sector, the periodicity of fermions in the base space is neither “naturally” periodic nor antiperiodic since there is a hole and branch cut from the twist operator; however, in the covering space, the fields are, again, naturally periodic.

We denote “bare twists” which insert the identity in the cover as

$$\sigma_p(z, \bar{z}) \xrightarrow[\text{cover}]{\text{to the}} \mathbb{1}(t, \bar{t}) \quad h = \bar{h} = \Delta_p = \frac{c}{24} \left(p - \frac{1}{p} \right). \quad (3.8)$$

After the above discussion, we see that one should always use

$$(\text{NS Sector}) \implies \begin{cases} \sigma_p(z, \bar{z}) & p \text{ odd} \\ S_p^\alpha(z) \bar{S}_p^{\dot{\alpha}}(\bar{z}) \sigma_p(z, \bar{z}) & p \text{ even} \end{cases}, \quad (\text{R Sector}) \implies S_p^\alpha(z) \bar{S}_p^{\dot{\alpha}}(\bar{z}) \sigma_p(z, \bar{z}). \quad (3.9)$$

The S_p 's indicate that one should insert a spin field in the p -fold covering space at the image of the point z . In the above statement, one could equally well choose $SU(2)_2$ indices instead of $SU(2)_{L/R}$ indices for the spin fields.

The CFT amplitude we compute uses the bare twists, which for odd twist order correspond to the NS sector and for even twist order correspond to neither the NS nor the R sector. Even though this amplitude is not physically relevant, we can use spectral flow to relate it to the R sector process of physical interest. Below, we give the initial and final states of the unphysical amplitude, starting with the simpler final state.

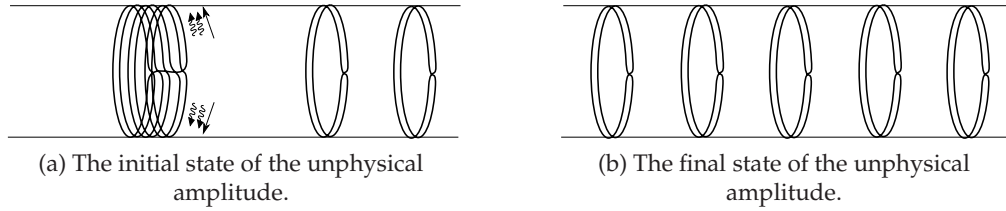


FIG. 3: The initial and final states of the unphysical amplitude. The initial state spectral flows to the physical final state, and the final state spectral flows to the physical initial state.

3.2. The final state

The *final* state¹ spectral flows to the *initial* state of the physical problem. All of the excitations and spin fields of the physical state can be acquired via spectral flow, so we use bare twists for the unphysical amplitude final state:

$$|f'\rangle = \underbrace{\sigma_\kappa \sigma_\kappa \cdots \sigma_\kappa}_{l+1} |\emptyset\rangle_{NS}. \quad (3.10)$$

This state has weight and charge

$$h_f = \bar{h}_f = \frac{1}{4}(l+1) \left(\kappa - \frac{1}{\kappa} \right) \quad m_f = \bar{m}_f = 0. \quad (3.11)$$

Note that for odd κ this state corresponds to the NS sector, but for κ even it corresponds to neither the NS nor the R sector. This state, which we call $|i\rangle$, is shown in Figure 3(b).

¹ Here, we just discuss the $\kappa(l+1)$ strands that are involved in the nontrivial part of the correlator. Later, we introduce the combinatoric factors which result from symmetrizing over all $N_1 N_5$ copies of the CFT.

3.3. The initial state

The *initial* state spectral flows to the physical final state, and therefore consists of excitations in the $\kappa(l+1)$ -twisted sector, as shown in Figure 3(a). Below, modulo normalization, we give the left part of the state

$$|i'\rangle = (J_0^-)^k G_{-\frac{1}{2\kappa}}^{-A} (L_{-\frac{1}{\kappa}})^N \psi_{-\frac{1}{2\kappa}}^{+\dot{A}} \begin{cases} J_{-\frac{l-1}{\kappa(l+1)}}^+ J_{-\frac{l-3}{\kappa(l+1)}}^+ \cdots J_{-\frac{1}{\kappa(l+1)}}^+ \sigma_{\kappa(l+1)} |\emptyset\rangle_{NS} & (l+1) \text{ odd} \\ J_{-\frac{l-1}{\kappa(l+1)}}^+ J_{-\frac{l-3}{\kappa(l+1)}}^+ \cdots J_{-\frac{2}{\kappa(l+1)}}^+ S_{\kappa(l+1)}^+ \sigma_{\kappa(l+1)} |\emptyset\rangle_{NS} & (l+1) \text{ even.} \end{cases} \quad (3.12)$$

The normalization of the state is κ -dependent, which plays an important role in the calculation as discussed in Section 7.2.

This state has weight and charge

$$h_i = \frac{1}{\kappa} \left(\frac{l}{2} + N + 1 \right) + \frac{1}{4}(l+1) \left(\kappa - \frac{1}{\kappa} \right) \quad m_i = \frac{l}{2} - k, \quad (3.13)$$

and similarly for the right sector. We conjecture the above form for the initial state based on the $\kappa = 1$ case in [1] and work done in [36] for $\kappa > 1$. The excited initial state should be dual to a supergravity excitation of the orbifolded-AdS background. In global AdS, one identifies the supergravity duals as the descendants of chiral primary states under the anomaly-free subalgebra; here, we propose the above modification for the κ -orbifolded background. This is motivated, in part, by the action of the vertex operator for absorption of supergravity particles on κ -orbifolded AdS.

3.4. The amplitude

The amplitude we compute, then, is

$$\mathcal{A}'^\kappa = \langle f' | \mathcal{V}_{l,l-k-\bar{k},k-\bar{k}}(z_2) | i' \rangle. \quad (3.14)$$

Note that if we map to the κ -cover, then these states are the initial and final states of the $\kappa = 1$ calculation in [1]. In mapping to a κ -covering space the final state's twist operators are removed, and the initial state's twist operator becomes an $(l+1)$ -twist. The J^+ modes acting on the initial state, along with the spin field for even $l+1$, act on the $(l+1)$ -twist in the κ -cover in precisely the correct way to form the lowest weight chiral primary twist operator of [53]:

$$J_{-\frac{l-1}{\kappa(l+1)}}^+ J_{-\frac{l-3}{\kappa(l+1)}}^+ \cdots \begin{cases} J_{-\frac{1}{\kappa(l+1)}}^+ \sigma_{\kappa(l+1)} \\ J_{-\frac{2}{\kappa(l+1)}}^+ S_{\kappa(l+1)}^+ \sigma_{\kappa(l+1)} \end{cases} \xrightarrow[\kappa\text{-cover}]{\text{to}} J_{-\frac{l-1}{l+1}}^+ J_{-\frac{l-3}{l+1}}^+ \cdots \begin{cases} J_{-\frac{1}{l+1}}^+ \sigma_{l+1} \\ J_{-\frac{2}{l+1}}^+ S_{l+1}^+ \sigma_{l+1} \end{cases} = \sigma_{l+1}^0. \quad (3.15)$$

We follow the notation of [1] by denoting the lowest weight chiral primary $(l+1)$ -twist operator, introduced in [53], as σ_{l+1}^0 . The above equation does not include Jacobian factors, computed in Sections 6 and 7, which are introduced in going to the κ -covering space.

The specific covering space to which we map preserves the form of the $(l+1)$ -twist vertex operator. The fact that going to a κ covering space gives the $\kappa = 1$ amplitude along with the gravity description of the emission process, is precisely the motivation for introducing the specific form of the state $|i'\rangle$.

4. RELATING THE COMPUTED CFT AMPLITUDE TO THE PHYSICAL PROBLEM

There are two steps needed to map the physical problem onto the unphysical CFT computation. First, we use spectral flow to map the physical states, $|i\rangle$ and $|f\rangle$, to the “primed states”, $|i'\rangle$ and $|f'\rangle$. Second, we use Hermitian conjugation to reverse the initial and final primed states.

4.1. Using spectral flow

We wish to relate a CFT amplitude computed with the unphysical “primed states”,

$$\mathcal{A}' = \langle f' | \mathcal{V}(z, \bar{z}) | i' \rangle, \quad (4.1)$$

to the physical amplitude in the Ramond sector. In this section, we show how to spectral flow [52, 54, 55] the physical problem in the R sector to the actual CFT amplitude we compute.

If spectral flowing the states $|i'\rangle$ and $|f'\rangle$ by α units is given by

$$|f'\rangle \mapsto |i\rangle = \mathcal{U}_\alpha |f'\rangle \quad \langle i' | \mapsto \langle f | = \langle i' | \mathcal{U}_{-\alpha}, \quad (4.2)$$

then we can compute the physical Ramond sector amplitude for emission of a particle with angular momentum (l, m_ψ, m_ϕ) by using

$$\begin{aligned} \mathcal{A}_{l, m_\psi, m_\phi} &= |z|^{l+2} \langle f | \mathcal{V}_{l, -m_\psi, -m_\phi}(z, \bar{z}) | i \rangle \\ &= |z|^{l+2} (\langle f | \mathcal{U}_\alpha) (\mathcal{U}_{-\alpha} \mathcal{V}_{l, -m_\psi, -m_\phi} \mathcal{U}_\alpha) (\mathcal{U}_{-\alpha} | i \rangle) \\ &= |z|^{l+2} \langle i' | \mathcal{V}'_{l, -m_\psi, -m_\phi}(z, \bar{z}) | f' \rangle. \end{aligned} \quad (4.3)$$

Note that one finds \mathcal{V}' by spectral flowing \mathcal{V} by $-\alpha$ units.

In [1], it was shown that the vertex operator transforms under spectral flow as

$$\mathcal{V}'_{l, l-k-\bar{k}, k-\bar{k}}(z, \bar{z}) = z^{-\alpha(\frac{l}{2}-k)} \bar{z}^{-\bar{\alpha}(\frac{l}{2}-\bar{k})} \mathcal{V}_{l, l-k-\bar{k}, k-\bar{k}}(z, \bar{z}). \quad (4.4)$$

We can use the vertex operator’s transformation to write

$$\mathcal{A}_{l, k+\bar{k}-l, \bar{k}-k} = z^{-\alpha(\frac{l}{2}-k)} \bar{z}^{-\bar{\alpha}(\frac{l}{2}-\bar{k})} |z|^{l+2} \langle i' | \mathcal{V}_{l, l-k-\bar{k}, k-\bar{k}}(z, \bar{z}) | f' \rangle. \quad (4.5)$$

Note that the primed states are reversed from what one would like.

The spectral flow parameter, α , is chosen to have a value that spectral flows the primed states to the physical states, which is achieved by

$$\alpha = 2n + \frac{1}{\kappa} \quad \bar{\alpha} = 2\bar{n} + \frac{1}{\kappa} \quad n, \bar{n} \in \mathbb{Z}. \quad (4.6)$$

Spectral flowing by non-integer units may seem strange, however, one can show that this results from the peculiar bare twist operators. Consider spectral flowing the bare twist σ_κ by $\frac{1}{\kappa}$ units, and recall that under spectral flow by α units

$$\beta_\pm \mapsto \beta_\pm \pm \alpha, \quad (4.7)$$

and

$$\beta_\pm^{(\text{cover})} = \kappa(\beta_\pm + 1) - 1. \quad (4.8)$$

The bare twist has $\beta_\pm^{(\text{cover})} = 0$, which after spectral flowing by $1/\kappa$ units becomes $\beta_\pm^{(\text{cover})} = 1$ consistent with the R boundary conditions in the base space. Similarly, one finds that the fermion periodicity of $|i'\rangle$ becomes correct for the R sector after spectral flowing by $1/\kappa$ units. After spectral flowing by $1/\kappa$ units to get to the R sector, we spectral flow by an even number of units to build up the fermionic excitations of the state $|i\rangle$.

4.2. Hermitian conjugation

Having related the physical amplitude to

$$\langle i' | \mathcal{V}_{l,m_\psi,m_\phi}(z,\bar{z}) | f' \rangle, \quad (4.9)$$

we now wish to switch the initial and final primed states by Hermitian conjugation.

On the cylinder, the vertex operator Hermitian conjugates as

$$\left[\tilde{\mathcal{V}}_{l,m_\psi,m_\phi}(\tau,\sigma) \right]^\dagger = \tilde{\mathcal{V}}_{l,-m_\psi,-m_\phi}(-\tau,\sigma), \quad (4.10)$$

and therefore

$$\langle i' | \tilde{\mathcal{V}}_{l,m_\psi,m_\phi}(\tau,\sigma) | f' \rangle = \left[\langle f' | \tilde{\mathcal{V}}_{l,-m_\psi,-m_\phi}(-\tau,\sigma) | i' \rangle \right]^\dagger. \quad (4.11)$$

In the complex plane, this statement translates to

$$|z|^{l+2} \langle i' | \mathcal{V}_{l,m_\psi,m_\phi}(z,\bar{z}) | f' \rangle = |z|^{-(l+2)} \left[\langle f' | \mathcal{V}_{l,-m_\psi,-m_\phi}\left(\frac{1}{z}, \frac{1}{\bar{z}}\right) | i' \rangle \right]^\dagger. \quad (4.12)$$

Applying this result to Equation (4.5), we may write the physical CFT amplitude for emission of a particle with angular momentum $(l, k + \bar{k}, \bar{k} - k)$ as

$$\begin{aligned} \mathcal{A}_{l,k+\bar{k}-l,\bar{k}-k} &= z^{-\alpha(\frac{l}{2}-k)} \bar{z}^{-\bar{\alpha}(\frac{l}{2}-\bar{k})} |z|^{-(l+2)} \left[\langle f' | \mathcal{V}_{l,k+\bar{k}-l,\bar{k}-k}\left(\frac{1}{z}, \frac{1}{\bar{z}}\right) | i' \rangle \right]^\dagger \\ &= z^{-\frac{l}{2}-1-\alpha(\frac{l}{2}-k)} \bar{z}^{-\frac{l}{2}-1-\bar{\alpha}(\frac{l}{2}-\bar{k})} \left[\mathcal{A}'_{l,k+\bar{k}-l,\bar{k}-k}\left(\frac{1}{z}, \frac{1}{\bar{z}}\right) \right]^\dagger. \end{aligned} \quad (4.13)$$

Thus, we compute the unphysical amplitude $\mathcal{A}'(z, \bar{z})$, and use the above relation to find the physical amplitude \mathcal{A} . The unphysical amplitude \mathcal{A}' is independent of k and \bar{k} , so we suppress the subscripts.

5. METHOD OF COMPUTATION

The way we compute the CFT amplitude \mathcal{A}'^κ is by noting that if one were to lift to the κ -cover, the amplitude becomes $\mathcal{A}'^{\kappa=1}$ computed in [1]. Specifically, if we transform to a coordinate u via the map

$$z = bu^\kappa \quad b = \frac{z_2}{u_2^\kappa}, \quad (5.1)$$

where u_2 is the image of the point z_2 ; then, the operators left in the correlator are exactly those for $\mathcal{A}'^{\kappa=1}$. In lifting to the cover, however, we do get some nontrivial ‘‘Jacobian factors’’ from the various operators in the correlator transforming under the map. Therefore, we write

$$\mathcal{A}'^\kappa = \left(\frac{\mathcal{A}'^\kappa}{\mathcal{A}'^{\kappa=1}} \right) \mathcal{A}'^{\kappa=1} = TM \mathcal{A}'^{\kappa=1}, \quad (5.2)$$

where we have written the Jacobian factors as the product of two contributions: one from the twists, T , and one from the modes, M .

We begin with the lengthier calculation of the nontrivial factor T that comes from the twist operators transforming. One can see that T is given by the ratio

$$T = \lim_{z_3 \rightarrow \infty} |z_3|^{4(l+1)\Delta_\kappa} \frac{\langle \sigma_\kappa \dots \sigma_\kappa(z_3) \sigma_{l+1}(z_2) \sigma_{\kappa(l+1)}(0) \rangle}{\langle \sigma_{l+1}(u_2) \sigma_{l+1}(0) \rangle}, \quad (5.3)$$

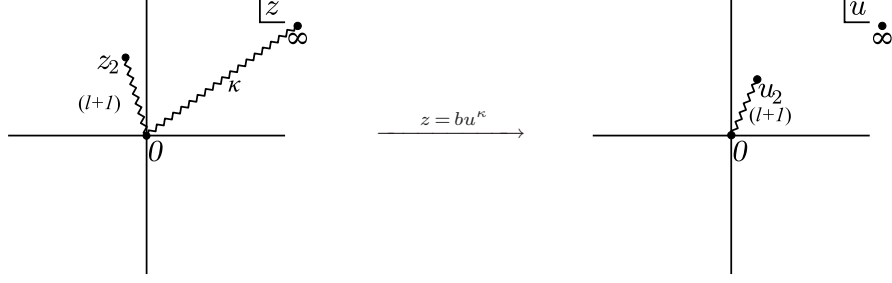


FIG. 4: In the z -plane, there is a twist operator of order $\kappa(l+1)$ at the origin, a twist of order $l+1$ at a point we call z_2 , and $l+1$ κ -twists at infinity. The diagram on the left depicts the branch cuts connecting the three points. The number next to the branch cut depicts its “order”. One can remove the $l+1$ branch cuts of order κ between the origin and infinity by mapping to the u -coordinate, as shown in the figure on the right.

where all of the above twists are “bare” twists which give *no* insertions in total $\kappa(l+1)$ -covering space. The z_3 prefactor ensures that in the limit as $z_3 \rightarrow \infty$ the $l+1$ twists at infinity make a normalized bra.

After computing T , we compute the mode Jacobian factor M , which is given by the product of all of the Jacobian factors that the modes circling the origin and the point z_2 acquire.

6. COMPUTING THE TWIST JACOBIAN FACTOR T

Since the *effect* of the twist operators is inherently nonlocal, they do not transform in a simple local way when lifting to a covering space. The simplest way to compute the numerator of Equation (5.3), is by lifting to the total covering space and then computing the Liouville action that comes in conformally transforming the induced metric on the covering space to a fiducial metric. This is the method developed in [46]. Recently, [56, 57] developed new technology for correlators of $S_{N_1 N_5}$ -twist operators; however, we do not use those techniques in this paper.

The denominator of Equation (5.3) is just the two-point function of some normalized twist operators, and so we know the answer:

$$\langle \sigma_{l+1}(u_2) \sigma_{l+1}(0) \rangle = \frac{1}{|u_2|^{\frac{\epsilon}{6}(l+1-\frac{1}{l+1})}} = \frac{1}{|u_2|^{4\Delta_{l+1}}}. \quad (6.1)$$

From the weights of the twist operators and $SL(2, \mathbb{C})$ invariance of the correlator, we know that any three-point function of quasi-primary fields must be given by

$$\begin{aligned} & \langle \mathcal{O}_3(z_3) \mathcal{O}_2(z_2) \mathcal{O}_1(z_1) \rangle \\ &= \frac{|C_{123}|^2}{(|z_1 - z_2|^{\Delta_1 + \Delta_2 - \Delta_3} |z_2 - z_3|^{\Delta_2 + \Delta_3 - \Delta_1} |z_3 - z_1|^{\Delta_3 + \Delta_1 - \Delta_2})^2}. \end{aligned} \quad (6.2)$$

In the present case where $z_3 = \infty$ and $z_1 = 0$, this gives (after regularizing the divergence which corresponds to correctly normalizing the final state)

$$\lim_{z_3 \rightarrow \infty} |z_3|^{4(l+1)\Delta_\kappa} \langle \sigma_\kappa \dots \sigma_\kappa(z_3) \sigma_{l+1}(z_2) \sigma_{\kappa(l+1)}(0) \rangle = \frac{|C|^2}{|z_2|^{2(\Delta_{\kappa(l+1)} + \Delta_{l+1} - (l+1)\Delta_\kappa)}}. \quad (6.3)$$

It is the constant C which is nontrivial and is determined in the calculation that follows. From the above, one sees that the twist Jacobian factor is completely determined by the constant C :

$$T = |C|^2 \frac{|u_2|^{4\Delta_{l+1}}}{|z_2|^{2(\Delta_{\kappa(l+1)} + \Delta_{l+1} - (l+1)\Delta_{\kappa})}}. \quad (6.4)$$

6.1. Review of method to compute correlators of twist operators

We use the methods developed in [46] to compute the correlator in Equation (6.3). We call the physical space where the problem is posed the “base space” which has the coordinates z and \bar{z} . In the base space, the basic fields are multivalued. The basic method to computing the correlators of twist operators consists of using a meromorphic mapping to a covering space where there is one set of single-valued fields. Having single-valued fields comes at the expense of introducing curvature in the covering space. Fortunately, we can conformally map the curved covering space to a manifold with metric in a fiducial (flat) form. Because of the conformal curvature anomaly, the path integral is not invariant under conformal mappings; however, the path integral changes in a specific way.

Suppose we compute the path integral of our conformal field theory on the manifold with fiducial metric \hat{ds}^2 , which we call \hat{Z} . The path integral of the same conformal field theory on a manifold with metric $ds^2 = e^\phi \hat{ds}^2$ which we call Z , is related to \hat{Z} by [58]

$$Z = e^{S_L} \hat{Z}, \quad (6.5)$$

where the Liouville action, S_L , is given by

$$S_L = \frac{c}{96\pi} \int d^2t \sqrt{-\hat{g}} \left[\hat{g}^{\mu\nu} \partial_\mu \phi \partial_\nu \phi + 2\hat{R}\phi \right]. \quad (6.6)$$

\hat{g} is the fiducial metric, and \hat{R} is the Ricci scalar of the *fiducial* metric.

We now outline the precise steps needed to compute correlators of twist operators, as given in [46]. The problem is posed in terms of some twist operators inserted at various points z_i in the base space. To make the fields well-defined, we cut a small hole of radius ε around each z_i and demand that the fields have the correct twisted boundary conditions around that hole. Furthermore, we regulate the path integral by putting the correlator on a disc of radius $1/\delta$, which encloses all of the z_i except twist operators that are inserted at infinity. To define the boundary conditions on the edge of the disc, we glue a second flat disc onto the edge of the first, giving the base space the topology of a sphere. Any twist operators located at infinity, we insert at the center of this second disc. We work on the base space with metric

$$ds^2 = \begin{cases} dzd\bar{z}, & |z| < \frac{1}{\delta} \\ d\tilde{z}d\bar{\tilde{z}}, & |\tilde{z}| < \frac{1}{\delta} \end{cases}, \quad \tilde{z} = \frac{1}{\delta^2} \frac{1}{z}. \quad (6.7)$$

The path integral with the various regularizations on the above metric we write as

$$Z_{\varepsilon, \delta}^{(s)}[\sigma_{n_1}(z_1) \cdots \sigma_{n_N}(z_N)]. \quad (6.8)$$

We can map to a covering space with metric ds'^2 with coordinates t and \bar{t} via a meromorphic function $z = z(t)$. Then, the path integral is given by

$$Z_{\varepsilon, \delta}^{(s)}[\sigma_{n_1}(z_1) \cdots \sigma_{n_N}(z_N)] = Z_{\varepsilon, \delta}^{(s')}, \quad (6.9)$$

where

$$ds^2 = dzd\bar{z} \implies ds'^2 = \frac{dz}{dt} \frac{d\bar{z}}{d\bar{t}} dt d\bar{t}. \quad (6.10)$$

When we write $Z^{(s')}$ with no square brackets we mean that there are no insertions in the path integral. Throughout this discussion, we assume that we are computing the correlator of bare twists which leave no insertions in the covering space. If this were not the case, then the right hand side of Equation (6.9) is multiplied by the separately computed correlator of those insertions in the covering space.

The sizes of the various holes in the t coordinates are determined by the mapping. The boundary conditions at the edges of the holes are defined by pasting in flat pieces of manifold in the covering space².

The induced metric on the covering space, ds'^2 , is conformally related to the fiducial metric we choose to work with

$$\hat{ds}^2 = \begin{cases} dt d\bar{t}, & |t| < \frac{1}{\delta'} \\ d\tilde{t} d\bar{\tilde{t}}, & |\tilde{t}| < \frac{1}{\delta'} \end{cases}, \quad \tilde{t} = \frac{1}{\delta'^2} \frac{1}{t}. \quad (6.11)$$

Thus, we can write

$$Z_{\varepsilon, \delta}^{(s)}[\sigma_{n_1}(z_1) \cdots \sigma_{n_N}(z_N)] = e^{S_L} Z_{\varepsilon, \delta, \delta'}^{(\hat{s})}. \quad (6.12)$$

The correlator of the regularized twist operators is defined by

$$\langle \sigma_{n_1}(z_1) \cdots \sigma_{n_N}(z_N) \rangle_{\varepsilon, \delta} = \frac{Z_{\varepsilon, \delta}^{(s)}[\sigma_{n_1}(z_1) \cdots \sigma_{n_N}(z_N)]}{(Z_\delta)^s} = e^{S_L} \frac{Z_{\varepsilon, \delta, \delta'}^{(\hat{s})}}{(Z_\delta)^s}, \quad (6.13)$$

where the s in the denominator is the number of Riemann sheets or the number of copies involved in the correlator (not to be confused with the metric). The path integral in the numerator, then, is also only over the twisted copies of the CFT, while the path integral with no insertions in the denominator, Z_δ , is the path integral of a single copy of the CFT with the metric in Equation (6.7).

The path integrals on the right-hand side of Equation (6.13) have no insertions and are on a metric of identical form. For the case where the covering space manifold has spherical topology, the path integrals cancel out up to the δ and δ' dependence.

To compute C in Equation (6.3) and thereby the twist Jacobian factor, T , we undertake the following steps:

1. We find the map to the total covering space, $z = z(t)$, that has the required properties.
2. We compute the Liouville action that comes from conformally mapping the induced metric of the total covering space to the fiducial form in Equation (6.11).
3. The above correlators are all of normalized twist operators. The normalization is such that the two-point function has unit correlator at unit separation, as determined in [46]. We put in the normalization factors, which cancel out the ε -dependence of the correlator.
4. Finally, we put all of the pieces together to determine C , and thereby T .

Step 2 we relegate to Appendix A.

² If the twist operators are not bare twists, then there would also be some operator insertions in the covering space; however, here we just discuss bare twists.

6.2. The map to the total covering space

The first step in the calculation of T , then, is to find the map to the total covering space. We have an $SL(2, \mathbb{C})$ symmetry of the covering space that allows us to fix three points. We fix the image of the origin of the z -plane to the origin of the t -plane, the image of z_2^3 to the point $t = 1$, and one image of $z = \infty$ to $t = \infty$. Having expended the $SL(2, \mathbb{C})$ symmetry, we do not have freedom to fix the locations of the other images of infinity in the covering space. We call the other images of infinity $t_\infty^{(j)}$, where $j = 1, \dots, l$.

Thus, we require our map to behave as

$$\begin{aligned} z &\sim t^{\kappa(l+1)} & z &\approx 0, t \approx 0 \\ z - z_2 &\sim (t - 1)^{l+1} & z &\approx z_2, t \approx 1 \\ z &\sim t^\kappa & z &\rightarrow \infty, t \rightarrow \infty \\ z &\sim (t - t_\infty^{(j)})^{-\kappa} & z &\rightarrow \infty, t \rightarrow t_\infty^{(j)}, \end{aligned} \tag{6.14}$$

and be regular at all other points. Here, \sim means proportional to at leading order. Generically, one expects $\kappa(l + 1)$ images of infinity. However, in this case there should only be $l + 1$ images of infinity since there are only $l + 1$ disconnected strings at $z \rightarrow \infty$. A priori, we do not know the $t_\infty^{(j)}$; this is part of the output in finding the map.

From the above conditions and requiring regularity everywhere but the above special points, we see that $\frac{dz}{dt}$ may have zeroes only at $t = 0$ (of degree $\kappa(l + 1) - 1$) and $t = 1$ (of degree l). Any meromorphic map can be written as the ratio of two polynomials,

$$z = \frac{f_1(t)}{f_2(t)}, \tag{6.15}$$

where f_1 must be of degree $\kappa(l + 1)$ and f_2 must be of degree κl , from the number of sheets and the behavior at infinity. Furthermore, near the origin we know that f_1 must behave as $t^{\kappa(l+1)}$ and f_2 a constant. Thus, we already have determined that

$$f_1 \propto t^{\kappa(l+1)}. \tag{6.16}$$

From familiarity with the two-point function map in [46] and consideration of the above requirements, one can immediately write down the correct map:

$$z = z_2 \frac{t^{\kappa(l+1)}}{[t^{l+1} - (t - 1)^{l+1}]^\kappa}. \tag{6.17}$$

Note that when $\kappa = 1$, the map reduces to the usual two-point map between 0 and z_2 ; and when $l = 0$, the map reduces to

$$z = z_2 t^\kappa, \tag{6.18}$$

which is the correct map for a two-point function between 0 and infinity. Furthermore, that the map is simply raising the two-point function map to the κ power makes sense, since when one

³ We should point out that there are other images of z_2 , but only $t = 1$ corresponds to where the vertex operator acts. The fact that there are other images of z_2 corresponds to the fact that the vertex operator only acts on $l + 1$ strands of the $\kappa(l + 1)$ initial strands.

goes to the κ -cover the correlator should become just the order $(l + 1)$ two-point function as depicted in Figure 4. The derivative of the map is

$$\frac{dz}{dt} = \frac{\kappa(l + 1)z_2}{[t^{l+1} - (t - 1)^{l+1}]^{\kappa+1}} t^{\kappa(l+1)-1} (t - 1)^l, \quad (6.19)$$

which has zeroes at the correct points. One can see from the map that it only has $l + 1$ distinct images of infinity, as required.

The behavior of the map near the irregular points is needed for the computation. Near the origin

$$z \approx (-1)^{\kappa l} z_2 t^{\kappa(l+1)} \quad \frac{dz}{dt} \approx (-1)^{\kappa l} \kappa(l + 1) z_2 t^{\kappa(l+1)-1}. \quad (6.20)$$

Near $t = 1$,

$$z \approx z_2 + z_2 \kappa (t - 1)^{l+1} \quad \frac{dz}{dt} \approx z_2 \kappa (l + 1) (t - 1)^l. \quad (6.21)$$

For large t ,

$$z \approx \frac{z_2}{(l + 1)^\kappa} t^\kappa \quad \frac{dz}{dt} \approx \frac{z_2 \kappa}{(l + 1)^\kappa} t^{\kappa-1}. \quad (6.22)$$

The images of infinity at finite t are the same as for the $l + 1$ order two-point map, that is

$$t_\infty^{(j)} = \frac{1}{1 - \alpha_j} \quad (\alpha_j)^{l+1} = 1, \quad (6.23)$$

where the α_j are the $(l + 1)$ roots of unity:

$$\alpha_j = e^{2\pi i \frac{j}{l+1}}. \quad (6.24)$$

Note that $\alpha_0 = 1$, which corresponds to $t \rightarrow \infty$; the case we already covered. Therefore, the images of infinity at finite t correspond to $j = 1, \dots, l$. If we let

$$t = \frac{1}{1 - \alpha_j} + x, \quad (6.25)$$

for small $x \in \mathbb{C}$, then near the images of infinity the map behaves as

$$z \approx (-1)^\kappa z_2 \left[\frac{\alpha_j}{(l + 1)(1 - \alpha_j)^2} \frac{1}{x} \right]^\kappa. \quad (6.26)$$

Plugging back in with t , one finds the behavior of the map near the finite images of infinity:

$$\begin{aligned} z &\approx (-1)^\kappa z_2 \left[\frac{\alpha_j}{(l + 1)(1 - \alpha_j)^2} \right]^\kappa \frac{1}{(t - t_\infty^{(j)})^\kappa} \\ \frac{dz}{dt} &\approx (-1)^{\kappa+1} \kappa z_2 \left[\frac{\alpha_j}{(l + 1)(1 - \alpha_j)^2} \right]^\kappa \frac{1}{(t - t_\infty^{(j)})^{\kappa+1}}. \end{aligned} \quad (6.27)$$

The map is regular at all other points not considered above.

In Appendix A, we use the local behavior of the map given above to compute the various contributions to the Liouville action.

6.3. Normalization

The regularized, but unnormalized three-point correlator is given by

$$\langle \underbrace{\sigma_{\kappa}^{\varepsilon} \cdots \sigma_{\kappa}^{\varepsilon}}_{l+1}(\infty) \sigma_{l+1}^{\varepsilon}(z_2) \sigma_{\kappa(l+1)}^{\varepsilon}(0) \rangle_{\delta} = e^{S_L} \frac{Z_{\delta'}^{(\hat{s})}}{(Z_{\delta})^{\kappa(l+1)}} = e^{S_L} Q^{1-\kappa(l+1)} \delta'^{-\frac{c}{3}} \delta^{\frac{c}{3}\kappa(l+1)}, \quad (6.28)$$

where for a sphere

$$Z_{\delta} = Q \delta^{-\frac{c}{3}} \quad Z_{\delta'}^{(\hat{s})} = Q \delta'^{-\frac{c}{3}}. \quad (6.29)$$

The factor Q is the path integral with the δ or δ' dependence, respectively, extracted. The fact that it is the same Q in both expressions is true only because we chose the fiducial covering space metric to be the same as the base space metric. One can see that the the path integral scales in this way from the curvature term of the Liouville action [46].

Note that instead of inserting the final state twists at a point z_3 in the finite z -plane and then taking a limit as in Equation (6.3), we have inserted the operators directly at “infinity” (the center of the second half of the t -sphere). As we shall see, the regularizing parameter $1/\delta$ plays the role of z_3 .

Calculations in Appendix A culminate in an expression for the total Liouville action,

$$\begin{aligned} S_L^{\text{tot.}} = & -\frac{c}{12} \left\{ \frac{(\kappa+1)l(l+2)}{\kappa(l+1)} \log |z_2| \right. \\ & - \frac{(l+2)^2}{l+1} \log \kappa - 4 \log(l+1) \\ & + \frac{1}{l+1} \left(l^2(\kappa+1) + 2l(\kappa-1) + \frac{(\kappa-1)^2}{\kappa} \right) \log \varepsilon \\ & + \frac{(l+1)(\kappa-1)^2}{\kappa} \log \tilde{\varepsilon} \\ & + \frac{2(l+1)(\kappa^2+1)}{\kappa} \log \delta \\ & \left. - 4 \log \delta' \right\}. \end{aligned} \quad (6.30)$$

Note that the δ' dependence of S_L cancels out with the δ' dependence in Equation (6.28), as it should. The total δ -dependence in Equation (6.28) is given by the power

$$\delta : \quad \frac{c}{6} \frac{(l+1)(\kappa^2-1)}{\kappa} = 4(l+1)\Delta_{\kappa}. \quad (6.31)$$

This power of δ gets cancelled out when demanding that the insertion of the twist operators at infinity make a properly normalized bra, as in Equation (6.3).

We want to compute the correlator for twist operators that are normalized such that their two-point function gives unity when they are unit separated in the z -plane. Normalizing the twists in the finite z -plane, we use the result from [46]:

$$\sigma_n = \frac{1}{\sqrt{C_n \varepsilon^{A_n} Q^{B_n}}} \sigma_n^{\varepsilon} = D_n \sigma_n^{\varepsilon}, \quad (6.32)$$

where

$$A_n = -\frac{c}{6} \frac{(n-1)^2}{n} \quad B_n = 1-n \quad C_n = n^{\frac{c}{3}}. \quad (6.33)$$

We normalize the twists at infinity in the same way, replacing ε by $\tilde{\varepsilon}$: at unit separation in their local coordinates they should have unit correlator with themselves. From Appendix B, we see that if we normalize the twists at infinity in this way, then

$$\langle \sigma_\kappa(\infty) \sigma_\kappa(0) \rangle_\delta = \delta^{4\Delta_\kappa}. \quad (6.34)$$

To ensure that the final state corresponds to a normalized bra, then, we should use

$$\lim_{z_3 \rightarrow \infty} |z_3|^{4\Delta_\kappa} \sigma_\kappa(z_3) = \delta^{-4\Delta_\kappa} \sigma_\kappa(\infty). \quad (6.35)$$

Thus, the δ dependence cancels out. Furthermore, once we normalize the twist operators the ε dependence drops out:

$$\varepsilon : \quad -\frac{c}{12} \frac{1}{l+1} \left(l^2(\kappa+1) + 2l(\kappa-1) + \frac{(\kappa-1)^2}{\kappa} \right) - \frac{1}{2}(A_{l+1} + A_{\kappa(l+1)}) = 0. \quad (6.36)$$

The $\tilde{\varepsilon}$ dependence also cancels out. Now, let's check the powers of Q :

$$Q : \quad 1 - \kappa(l+1) + \frac{l}{2} + \frac{\kappa(l+1)-1}{2} + \frac{(\kappa-1)(l+1)}{2} = 0; \quad (6.37)$$

there is no Q -dependence left and so we never have to actually compute the path integral. One can show that the Q -dependence always cancels out for correlators with spherical covering spaces.

One finds that the powers of $(l+1)$ cancel out as well. The constant C , then, is given as a power of κ :

$$|C|^2 = \kappa^{-\frac{c}{12} \frac{l(l+2)}{l+1}}. \quad (6.38)$$

The power of κ may seem mysterious, until one realizes that

$$\Delta_{l+1} = \frac{c}{24} \left(l+1 - \frac{1}{l+1} \right) = \frac{1}{4} \frac{l(l+2)}{l+1},$$

and so we write

$$|C|^2 = \kappa^{-2\Delta_{l+1}}. \quad (6.39)$$

6.4. The twist jacobian factor T

Plugging in the value of C into Equation (6.4), one finds the twist Jacobian factor,

$$T = \kappa^{-2\Delta_{l+1}} \frac{|u_2|^{4\Delta_{l+1}}}{|z_2|^{2\frac{\kappa+1}{\kappa}\Delta_{l+1}}}. \quad (6.40)$$

Note that this Jacobian factor cannot naturally be thought of as the product of Jacobian factors from the different twist operators. This fact is what makes correlation functions of twist operators nontrivial.

7. COMPUTING THE MODE JACOBIAN FACTOR M

To compute the mode Jacobian factor, M , we first illustrate how modes transform under the map $z = bu^\kappa$. Then, we compute the mode Jacobian factor from the initial state modes, followed by the mode Jacobian factor from the vertex operator modes. The final state does not have any modes, and therefore does not contribute to M . In discussing the initial state, we find that we must also consider the κ -dependence of the normalization of the state.

7.1. Transformation law for modes

First, let us examine how the different modes transform under the map,

$$z = bu^\kappa. \quad (7.1)$$

Modes that circle the origin get opened up by a factor of κ , and also get a Jacobian factor. They transform as

$$\mathcal{O}_m^{(z)} = b^m \kappa^{1-\Delta} \mathcal{O}_{m\kappa}^{(u)}, \quad (7.2)$$

where Δ is the weight of the field $\mathcal{O}(z)$. One can see this from the definition of modes in the $\kappa(l+1)$ -twisted sector [53]:

$$\mathcal{O}_{\frac{m}{\kappa(l+1)}}^{(z)} = \oint \frac{dz}{2\pi i} \sum_{j=1}^{\kappa(l+1)} \mathcal{O}_{(j)}(z) e^{2\pi i \frac{m}{\kappa(l+1)}(j-1)} z^{\Delta-1+\frac{m}{\kappa(l+1)}}. \quad (7.3)$$

The subscripted parenthetical index on the field $\mathcal{O}_{(j)}$ denotes the copy the field lives on.

Modes which circle z_2 , where there is no branching point, transform as

$$\mathcal{O}_m^{(z)} = \left(\frac{dz}{du} \Big|_{u_2, z_2} \right)^m \mathcal{O}_m^{(u)}. \quad (7.4)$$

Near the point u_2 , the map behaves as

$$\begin{aligned} z &\approx z_2 + \kappa b u_2^{\kappa-1} (u - u_2) \\ &= z_2 + \kappa \frac{z_2}{u_2} (u - u_2). \end{aligned} \quad (7.5)$$

Therefore, we see that, under this map, modes which circle the point z_2 transform as

$$\mathcal{O}_m^{(z)} = \left(\kappa \frac{z_2}{u_2} \right)^m \mathcal{O}_m^{(u)}. \quad (7.6)$$

Since the spectral flowed final state does not have any modes, we can write M as a product of Jacobian factors from the initial state and Jacobian factors from the vertex operator,

$$M = M_i M_v. \quad (7.7)$$

7.2. The mode jacobian factor from the initial state

For the initial state, we need to be a little careful about the normalization. Consider an initial state defined in the base space as

$$|\psi^{(z)}\rangle = \mathcal{C} \mathcal{O}_m^{(z)} |\sigma_{\kappa(l+1)}\rangle. \quad (7.8)$$

The norm of this state is given by

$$\begin{aligned} \langle \psi^{(z)} | \psi^{(z)} \rangle &= |\mathcal{C}|^2 \langle \sigma_{\kappa(l+1)} | \mathcal{O}_{-m}^{\dagger(z)} \mathcal{O}_m^{(z)} | \sigma_{\kappa(l+1)} \rangle \\ &= |\mathcal{C}|^2 \langle \sigma_{l+1} | \left(b^{-m} \kappa^{1-\Delta} \mathcal{O}_{-m\kappa}^{\dagger(u)} \right) \left(b^m \kappa^{1-\Delta} \mathcal{O}_{m\kappa}^{(u)} \right) | \sigma_{l+1} \rangle \\ &= |\mathcal{C}|^2 \kappa^{2(1-\Delta)} \langle \sigma_{l+1} | \mathcal{O}_{-m\kappa}^{\dagger(u)} \mathcal{O}_{m\kappa}^{(u)} | \sigma_{l+1} \rangle. \end{aligned} \quad (7.9)$$

On the other hand, suppose one were to define the state directly in the cover as

$$|\psi^{(u)}\rangle = \mathcal{C}_{\text{cover}} \mathcal{O}_{m\kappa}^{(u)} |\sigma_{l+1}\rangle, \quad (7.10)$$

then its norm is given by

$$\langle \psi^{(u)} | \psi^{(u)} \rangle = |\mathcal{C}_{\text{cover}}|^2 \langle \sigma_{l+1} | \mathcal{O}_{-m\kappa}^{\dagger(u)} \mathcal{O}_{m\kappa}^{(u)} | \sigma_{l+1} \rangle. \quad (7.11)$$

Requiring that both $|\psi^{(z)}\rangle$ and $|\psi^{(u)}\rangle$ be normalized, means

$$\mathcal{C} = \frac{\mathcal{C}_{\text{cover}}}{\kappa^{1-\Delta}}. \quad (7.12)$$

Thus, using Equation (7.2) with Equation (7.8), one finds

$$|\psi^{(z)}\rangle = b^m |\psi^{(u)}\rangle. \quad (7.13)$$

From this we see that the κ factor in Equation (7.2) gets cancelled out by the κ s one gets in normalizing the state in the covering space. This argument easily generalizes to all of the modes acting in the initial state.

The only contributions to M_i , therefore, come from the factors b^m . Because of the way they come in, we see that the the total factor we get (from the left) is

$$b^{-h_i^{\text{modes}}}, \quad (7.14)$$

where h_i^{modes} is the weight of all of the modes in the initial state. This is simply the total weight of the initial state minus the weight of the bare twist:

$$\begin{aligned} h_i^{\text{modes}} &= h'_i - \Delta_{\kappa(l+1)} \\ &= \frac{l+1}{4} \left(\kappa - \frac{1}{\kappa} \right) + \frac{1}{\kappa} \left(\frac{l}{2} + 1 \right) + \frac{N}{\kappa} - \frac{1}{4} \left(\frac{\kappa(l+1)}{\kappa(l+1)} - \frac{1}{\kappa(l+1)} \right) \\ &= \frac{1}{\kappa} \left[\frac{l}{2} + N + 1 - \Delta_{l+1} \right]. \end{aligned} \quad (7.15)$$

Therefore, the total contribution (including both the left and right sectors) to the mode Jacobian factor from the initial state is given by

$$\begin{aligned} M_i &= |b|^{-\frac{2}{\kappa} [\frac{l}{2} + 1 - \Delta_{l+1}]} b^{-\frac{N}{\kappa}} \bar{b}^{-\frac{\bar{N}}{\kappa}} \\ &= \frac{|u_2|^2 [\frac{l}{2} + 1 - \Delta_{l+1}]}{|z_2|^{\frac{2}{\kappa} [\frac{l}{2} + 1 - \Delta_{l+1}]}} \frac{u_2^N \bar{u}_2^{\bar{N}}}{z_2^{\frac{N}{\kappa}} \bar{z}_2^{\frac{\bar{N}}{\kappa}}}. \end{aligned} \quad (7.16)$$

7.3. The mode jacobian factor from the vertex operator

The vertex operator, we can see from

$$\mathcal{O}_m^{(z)} = \left(\kappa \frac{z_2}{u_2} \right)^m \mathcal{O}_m^{(t)},$$

contributes a factor of

$$M_v = \left(\kappa \frac{z_2}{u_2} \right)^{-h_v^{\text{modes}}} \left(\kappa \frac{\bar{z}_2}{\bar{u}_2} \right)^{-\bar{h}_v^{\text{modes}}}, \quad (7.17)$$

where h_v^{modes} is the weight of the vertex operator less the weight of the bare $(l+1)$ -twist, that is,

$$h_v^{\text{modes}} = \bar{h}_v^{\text{modes}} = \frac{l}{2} + 1 - \Delta_{l+1}. \quad (7.18)$$

Therefore, we see that the contribution to the mode Jacobian factor from the vertex operator is given by

$$M_v = \kappa^{2\Delta_{l+1}-(l+2)} \left(\frac{|u_2|}{|z_2|} \right)^{l+2-2\Delta_{l+1}}. \quad (7.19)$$

8. THE CFT AMPLITUDE

Multiplying the mode Jacobian factor,

$$M = M_i M_v = \kappa^{2\Delta_{l+1}-(l+2)} \frac{|u_2|^{2(l+2)-4\Delta_{l+1}}}{|z_2|^{\frac{\kappa+1}{\kappa}[l+2-2\Delta_{l+1}]}} \frac{u_2^N \bar{u}_2^{\bar{N}}}{z_2^{\frac{N}{\kappa}} \bar{z}_2^{\frac{\bar{N}}{\kappa}}}, \quad (8.1)$$

with the twist Jacobian factor,

$$T = \kappa^{-2\Delta_{l+1}} \frac{|u_2|^{4\Delta_{l+1}}}{|z_2|^{2\frac{\kappa+1}{\kappa}\Delta_{l+1}}},$$

one finds

$$TM = \kappa^{-(l+2)} \frac{|u_2|^{2(l+2)}}{|z_2|^{\frac{\kappa+1}{\kappa}(l+2)}} \frac{u_2^N \bar{u}_2^{\bar{N}}}{z_2^{\frac{N}{\kappa}} \bar{z}_2^{\frac{\bar{N}}{\kappa}}}. \quad (8.2)$$

Finally, from [1] we take the $\kappa = 1$ CFT amplitude (before spectral flow and *without Jacobian prefactor* $|z|^{l+2}$ from mapping from the cylinder to the complex plane)

$$\mathcal{A}'^{\kappa=1} = (-1)^{k+\bar{k}} \sqrt{\binom{N+l+1}{N} \binom{\bar{N}+l+1}{\bar{N}}} \frac{1}{|u_2|^{2(l+2)} u_2^N \bar{u}_2^{\bar{N}}}, \quad (8.3)$$

and use the Jacobian factor TM to find

$$\mathcal{A}'^{\kappa}(z_2, \bar{z}_2) = \kappa^{-(l+2)} \sqrt{\binom{N+l+1}{N} \binom{\bar{N}+l+1}{\bar{N}}} \frac{1}{|z_2|^{\frac{\kappa+1}{\kappa}(l+2)} z_2^{\frac{N}{\kappa}} \bar{z}_2^{\frac{\bar{N}}{\kappa}}}, \quad (8.4)$$

which reduces to Equation (8.3) for $\kappa = 1$.

9. COMBINATORICS

As in [1], we want to consider an initial state with ν excitations that de-excites into a final states with $\nu - 1$ excitations (shown in Figure 5); however, the background geometry now consists of κ -twisted component strings. We assume, therefore, that κ divides $N_1 N_5$. Because the theory is orbifolded by $S_{N_1 N_5}$, the initial state, the final state, and the vertex operator must all be symmetrized over the $N_1 N_5$ copies.

We relate the full symmetrized states and operator to the amplitude computed above, in which we do not worry about these combinatoric factors. The combinatorics for this problem are quite similar to and for $\kappa = 1$ reduce to the combinatorics in [1].

9.1. The initial state

We write the initial state as a sum over all the symmetric permutations:

$$|\Psi_\nu\rangle = \mathcal{C}_\nu \left[|\psi_\nu^1\rangle + |\psi_\nu^2\rangle + \dots \right], \quad (9.1)$$

where \mathcal{C}_ν is the overall normalization and each $|\psi_\nu^i\rangle$ is individually normalized. The initial state for $\nu = 2$, $\kappa = 2$, and $l = 2$ is shown in Figure 5(a).

To understand what we are doing better, note that the state $|\psi_{\nu=2}^1\rangle$ with $\kappa = 2$ and $l + 1 = 3$ can be written schematically as

$$|\psi_\nu^1\rangle = |[1 \cdots 6] [7 \cdots 12] [12, 13] [14, 15] \cdots\rangle \quad (9.2)$$

where the numbers in the square brackets are indicating particular ways of twisting individual strands corresponding to particular cycles of the permutation group. For instance,

$$|[1234]\rangle, \quad (9.3)$$

indicates that we twist strand 1 into strand 2 into strand 3 into strand 4 into strand 1 and leave strands 5 through $N_1 N_5$ untwisted. In Equation (9.2), the first two 6-twists are the two $\kappa(l + 1)$ -twists which indicate the two excitations; the remaining $(\kappa = 2)$ -twists correspond to the background.

To determine the normalization \mathcal{C}_ν , we need to count the number of distinct terms in Equation (9.1). To count the number of states, we imagine constructing one of the terms and count how many choices we have. First, of the $N_1 N_5$ strands we must pick $\nu\kappa(l + 1)$ of them to make into the ν excited states. Next, we must break the $\nu\kappa(l + 1)$ strands into sets of $\kappa(l + 1)$ to be twisted together. Then, we must pick a way of twisting together each set of $\kappa(l + 1)$. Finally, we must make similar choices for the $N_1 N_5 - \nu\kappa(l + 1)$ strands that are broken into the κ -twists of the background. Putting these combinatoric factors together, one finds

$$\begin{aligned} N_{\text{terms}} &= \binom{N_1 N_5}{\nu\kappa(l + 1)} \\ &\quad \times \binom{\nu\kappa(l + 1)}{\kappa(l + 1)} \binom{(\nu - 1)\kappa(l + 1)}{\kappa(l + 1)} \cdots \binom{\kappa(l + 1)}{\kappa(l + 1)} \frac{1}{\nu!} \times ([\kappa(l + 1) - 1]!)^\nu \\ &\quad \times \binom{N_1 N_5 - \nu\kappa(l + 1)}{\kappa} \cdots \binom{\kappa}{\kappa} \frac{1}{[\frac{N_1 N_5}{\kappa} - \nu(l + 1)]!} \times ((\kappa - 1)!)^{\frac{N_1 N_5}{\kappa} - \nu(l + 1)} \\ &= \frac{(N_1 N_5)!}{[\kappa(l + 1)]^\nu \kappa^{\frac{N_1 N_5}{\kappa} - \nu(l + 1)} (\frac{N_1 N_5}{\kappa} - \nu(l + 1))! \nu!}. \end{aligned} \quad (9.4)$$

Choosing \mathcal{C}_ν to be real, one finds

$$\mathcal{C}_\nu = \frac{1}{\sqrt{N_{\text{terms}}}} = \left[\frac{(N_1 N_5)!}{[\kappa(l + 1)]^\nu \kappa^{\frac{N_1 N_5}{\kappa} - \nu(l + 1)} (\frac{N_1 N_5}{\kappa} - \nu(l + 1))! \nu!} \right]^{-\frac{1}{2}}. \quad (9.5)$$

9.2. The final state

The final state is simply $|\Psi_{\nu-1}\rangle$ with its corresponding normalization $\mathcal{C}_{\nu-1}$. This state is shown for $\nu = 2$, $\kappa = 2$, and $l = 2$ in Figure 5(b).

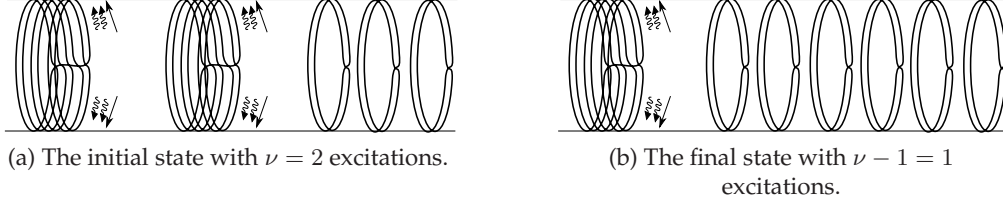


FIG. 5: The initial and final states of the unphysical amplitude with some excitations present in the background. An $l = 2$ transition from $\nu = 2$ excitations to 1 excitation of the $\kappa = 2$ background is shown.

9.3. The vertex operator

The normalization of the vertex operator was determined in [1]. The full symmetrized vertex operator is written

$$\mathcal{V}_{\text{sym}} = \mathcal{C} \sum_i \mathcal{V}_i, \quad (9.6)$$

where

$$\mathcal{C} = \left[\frac{(N_1 N_5)!}{(l+1)[N_1 N_5 - (l+1)]!} \right]^{-\frac{1}{2}}. \quad (9.7)$$

9.4. The amplitude

The full amplitude of interest is

$$\langle \Psi_{\nu-1} | \mathcal{V}_{\text{sym}} | \Psi_{\nu} \rangle, \quad (9.8)$$

which we wish to relate to a “single” unsymmetrized amplitude. Having the normalization of the initial state, the final state, and the vertex operator, all that remains is to determine which terms in the symmetrized states and operator combine to give a nonzero amplitude. For each initial state there are ν excitations that a term in the vertex operator can de-excite. We are left with the question, how many $(l+1)$ -twists can untwist a given $\kappa(l+1)$ -twist into $l+1$ κ -twists? In fact, there are κ such twist operators, which brings the number of nonzero amplitudes to

$$N_{\text{terms}} \nu \kappa = \kappa \frac{\nu}{\mathcal{C}_{\nu}^2}. \quad (9.9)$$

To illustrate, consider the initial state in Equation (9.2) for $\nu = 2$, $\kappa = 2$, and $l+1 = 3$. First, there are two different excitations to untwist. Consider untwisting the first excitation [123456]. There are exactly two 3-twist vertex operators that untwist the excitation into three sets of 2-twists: [531] and [642]. The [531] vertex operator breaks the initial state into [12][34][56], while the [642] vertex operator breaks the initial state into [61][23][45].

Using Equation (9.9) and the normalizations, we can relate the total symmetrized amplitude to the amplitude computed with only one term from the initial state, the final state, and the vertex operator:

$$\begin{aligned} \langle \Psi_{\nu-1} | \mathcal{V}_{\text{sym}} | \Psi_{\nu} \rangle &= \mathcal{C}_{\nu-1} \mathcal{C}_{\nu} \kappa \frac{\nu}{\mathcal{C}_{\nu}^2} \langle \psi_{\nu-1}^1 | \mathcal{V}_1 | \psi_{\nu}^1 \rangle \\ &= \sqrt{\kappa^{l+2\nu} \frac{[\frac{N_1 N_5}{\kappa} - (\nu-1)(l+1)]! [N_1 N_5 - (l+1)]!}{[\frac{N_1 N_5}{\kappa} - \nu(l+1)]! (N_1 N_5)!}} \langle \psi_{\nu-1}^1 | \mathcal{V}_1 | \psi_{\nu}^1 \rangle. \end{aligned} \quad (9.10)$$

9.5. The large $N_1 N_5$ limit

While the expression in Equation (9.10) is complicated, it simplifies considerably in the large $N_1 N_5$ limit of ultimate interest. We take both $N_1 N_5$ and $N_1 N_5 / \kappa$ to be large,

$$\frac{[\frac{N_1 N_5}{\kappa} - (\nu - 1)(l + 1)]!}{[\frac{N_1 N_5}{\kappa} - \nu(l + 1)]!} \longrightarrow \left(\frac{N_1 N_5}{\kappa}\right)^{(l+1)} \quad \frac{[N_1 N_5 - (l + 1)]!}{(N_1 N_5)!} \longrightarrow (N_1 N_5)^{-(l+1)}, \quad (9.11)$$

in which case Equation (9.10) reduces to

$$\langle \Psi_{\nu-1} | \mathcal{V}_{\text{sym}} | \Psi_{\nu} \rangle = \sqrt{\kappa \nu} \langle \psi_{\nu-1}^1 | \mathcal{V}_1 | \psi_{\nu}^1 \rangle. \quad (9.12)$$

The $\sqrt{\nu}$ prefactor can be thought of as a “Bose enhancement” effect.

10. THE RATE OF EMISSION

We now can put all of the pieces together to find the spectrum and rate of emission. Plugging Equation (8.4) into Equation (4.13) along with the combinatoric factors from Equation (9.12), one finds the amplitude for emission with angular momentum $(l, k + \bar{k} - l, \bar{k} - k)$

$$\mathcal{A}_{l, k + \bar{k} - l, \bar{k} - k} = \sqrt{\nu \kappa} \kappa^{-(l+2)} \sqrt{\binom{N + l + 1}{N} \binom{\bar{N} + l + 1}{\bar{N}}} z^{\frac{1}{\kappa}(\frac{l}{2} + N + 1) - \alpha(\frac{l}{2} - k)} \bar{z}^{\frac{1}{\kappa}(\frac{l}{2} + \bar{N} + 1) - \bar{\alpha}(\frac{l}{2} - \bar{k})}. \quad (10.1)$$

Plugging back in with the physical cylindrical coordinates,

$$z = e^{\frac{i}{R}(y+t)} \quad \bar{z} = e^{-\frac{i}{R}(y-t)}, \quad (10.2)$$

we can read off the spectrum for emission,

$$\begin{aligned} E_0 &= \frac{1}{\kappa R} [(\kappa \alpha + \kappa \bar{\alpha} - 2)\frac{l}{2} - \kappa(\alpha k + \bar{\alpha} \bar{k}) - N - \bar{N} - 2] \\ \lambda_0 &= \frac{1}{\kappa R} [-\kappa(\alpha - \bar{\alpha})\frac{l}{2} + \kappa(\alpha k - \bar{\alpha} \bar{k}) + N - \bar{N}], \end{aligned} \quad (10.3)$$

where recall that $\alpha = 2n + 1/\kappa$ and $\bar{\alpha} = 2\bar{n} + 1/\kappa$. For there to be emission the energy of the emitted particle must be positive, meaning that $E_0 > 0$.

The unit amplitude with the (σ, τ) dependence removed is

$$\mathcal{A}_{\text{unit}}(0) = \sqrt{\nu \kappa}^{-l - \frac{3}{2}} \sqrt{\binom{N + l + 1}{N} \binom{\bar{N} + l + 1}{\bar{N}}}. \quad (10.4)$$

Section 9, where ν is defined, calculates the combinatorics for the *unphysical* amplitude. For the *physical* amplitude, the combinatorics are the same except that the emission process is a transition from $\nu - 1$ to ν $\kappa(l + 1)$ -twists. Thus, the above is the amplitude for emission of the ν th particle. Plugging into Equation (1.2), one finds the emission rate for the ν th particle,

$$\frac{d\Gamma}{dE} = \nu \kappa^{-2l-3} \frac{2\pi}{2^{2l+1} l!^2} \frac{(Q_1 Q_5)^{l+1}}{R^{2l+3}} (E^2 - \lambda^2)^{l+1} \binom{N + l + 1}{N} \binom{\bar{N} + l + 1}{\bar{N}} \delta_{\lambda, \lambda_0} \delta(E - E_0), \quad (10.5)$$

with energy and momentum in Equation (10.3) and angular momentum $(l, k + \bar{k} - l, \bar{k} - k)$. This answer exactly matches the gravity calculation in [36].

11. DISCUSSION

We reproduced the full spectrum and emission rate of supergravity minimal scalars from the geometries found in [2] by using a CFT formalism. In [36, 48, 49], using a heuristic picture of the CFT process the spectrum and rate was found, but only for special cases ($N = \bar{N} = 0$ and $k = \bar{k} = 0$) and the normalization of the heuristic vertex operator was determined only indirectly. In [1], the full rate and spectrum was found as a rigorous calculation for $\kappa = 1$ with a vertex operator whose coupling to flat space and normalization was determined directly from the AdS/CFT correspondence.

The new feature of this paper from results found in [1] is the κ -dependence. Using the old effective string description, the κ -dependence in Equations (10.3) and (10.5) could have been guessed via a heuristic argument that we now describe. Taking higher values of κ corresponds to twisting the background strings by κ . The process, then, looks the same as for $\kappa = 1$ but taking $R \mapsto \kappa R$. This reproduces the explicit κ dependence of Equation (10.5), but the spectrum is slightly more complicated. In the spectrum, we also should take $R \mapsto \kappa R$, since the energy level spacing becomes reduced by a factor of κ ; however, things are complicated by the parameters n and \bar{n} . Why does the n and \bar{n} part of the spectrum get multiplied by κ with respect to the rest of the contributions to the energy? The parameters n and \bar{n} control the Fermi level of the physical initial state. In the κ -cover, the fermions fill up to energy level κn and not n ; thus, the extra factor of κ .

With the final answer and CFT computation in front of us, this heuristic argument seems compelling indeed; however, we argue that it is not completely obvious a priori that the effective string reasoning works for this calculation. Certainly, the way that the κ -dependence works out in the rigorous CFT calculation seems quite nontrivial and nonobvious. That the action of the vertex operator so simply just gets “divided by” κ does not seem obvious. In any case, one of our goals in this paper is to demonstrate the formalism in [1] and put the reasoning in [36, 48, 49] on a firmer footing. Along the way, we found the form of supergravity excitations on the orbifolded-AdS background; it would be nice to better understand the identification of the supergravity multiplet in orbifolded-AdS.

That the rate of emission computed in this class of geometries can be reproduced via a CFT calculation may seem insignificant in the face of so many AdS/CFT successes. There are two reasons why this calculation is of interest. First, most AdS/CFT calculations use a gravity calculation in the AdS to compute a CFT correlator, whereas we use [1] to compute the rate of emission *out of the CFT or AdS*. This demonstrates the formalism of [1], which hearkens back to and puts a firmer footing on the “effective string” calculations of [59, 60, 61, 62, 63, 64]. Second, as explained in [36, 48, 49], the CFT calculation justifies interpreting the ergoregion emission as Hawking radiation from these, albeit nongeneric, microstates of a black hole. This may help us better understand black holes in string theory and thereby quantum gravity.

All of the calculations in this paper were performed on the “orbifold point” of the D1D5 CFT. The emission process described in the gravity side should be dual to the CFT off of the orbifold point, and so it is an open question why this and many other calculations on the orbifold point so accurately reproduce the gravitational physics. In the future, we plan to move off of the orbifold point in the hope that we can answer this and many dynamical questions about black holes.

Acknowledgments

We are very grateful for S. Mathur’s insights, guidance, and helpful discussions over the course of this project. We also thank Y. Srivastava and P. Kraus for conversations and comments.

This work was supported in part by DOE grant DE-FG02-91ER-40690.

APPENDIX A: COMPUTING THE LIOUVILLE ACTION

The correct way to define the correlator in Equation (6.3) is to cut holes in the z plane around $z = 0$ and $z = z_2$ of size ε and then a large cut at $|z| = 1/\delta$. The small holes around the origin and z_2 have the appropriate boundary conditions for the twist operators. Upon the cut at $|z| = 1/\delta$, we glue a second flat disc with coordinate \tilde{z} . The center of this second disc has a hole of size $\tilde{\varepsilon}$, which has the boundary conditions appropriate for the $(l + 1)$ κ -twists at infinity. The metric on this manifold is

$$ds^2 = \begin{cases} dzd\bar{z} & |z| < \frac{1}{\delta} \\ d\tilde{z}d\bar{\tilde{z}} & |\tilde{z}| < \frac{1}{\delta} \end{cases} \quad (A.1)$$

$$z = \frac{1}{\delta^2 \tilde{z}}.$$

Note that there is a ring of curvature at $|z| = 1/\delta$. The base space with holes is pictured in Figure 6.

We map to a covering space with coordinates t and \bar{t} using the map given in Equation (6.17). The manifold still has holes from the images of the twist operators. We close all of the holes in the manifold by pasting in flat patches. Then, the covering space manifold, which we call Σ , becomes compact with the topology of a sphere⁴. The $l + 1$ κ -twist operators which corresponded to a single hole in the base space at $\tilde{z} = 0$ map to $l + 1$ different holes in the covering space, l in the finite t plane and one at infinity. These holes we also close with flat patches. The covering space is pictured in Figure 6.

The metric induced on the manifold Σ from the base metric (A.1) is conformally related to the fiducial metric for the t -sphere,

$$\hat{ds}^2 = \begin{cases} dt d\bar{t} & |t| < \frac{1}{\delta'} \\ d\tilde{t} d\bar{\tilde{t}} & |\tilde{t}| < \frac{1}{\delta'} \end{cases} \quad (A.2)$$

$$t = \frac{1}{\delta'^2 \tilde{t}}.$$

We choose δ' such that the outermost image of $|z| = \frac{1}{\delta}$ is contained in the first half of the t -sphere.

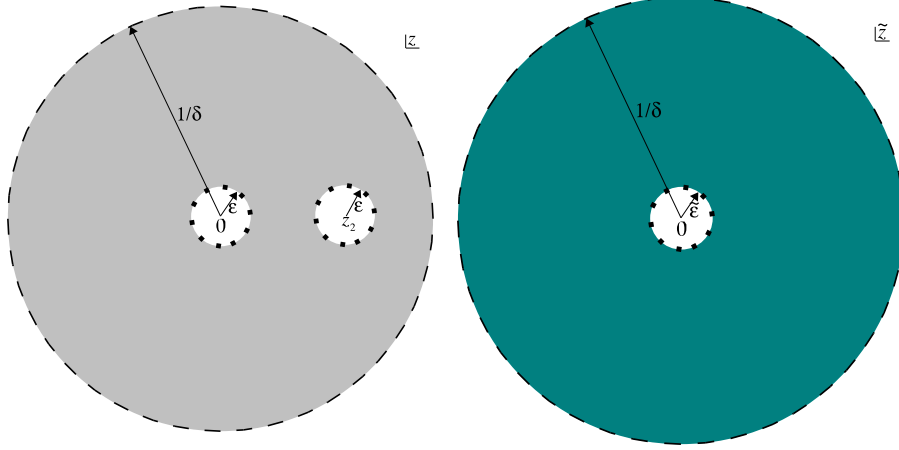
Note that unlike the calculations performed in [46], for our map all $(l + 1)$ images of infinity correspond to a distinct twist operator inserted at infinity in the base space.

The Liouville field ϕ is defined by

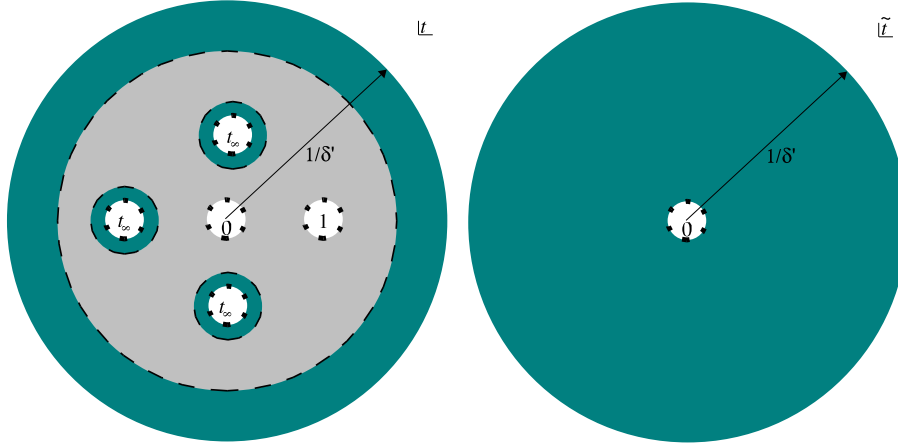
$$ds^2 = e^\phi \hat{ds}^2. \quad (A.3)$$

We break the manifold Σ into a “regular region”, which is the image of the “first half” of the z -sphere with the holes cut out; the “annuli”, which consist of the images of the second half of the z -sphere with the hole around $\tilde{z} = 0$ cut out; the “second half” of the t -sphere with the hole cut out; and finally, the flat patches which we pasted in to make the manifold compact. Using this

⁴ For the specific correlator we compute, the Riemann–Hurwitz formula determines that the covering space has genus zero. In other cases, one can get higher genus covering spaces, as discussed in [46].



(a) The regularized z -sphere.



(b) The t -sphere for $l = 3$.

FIG. 6: This figure shows how the base space, where the correlator is defined, gets mapped to the covering space. The “first half” of the z -sphere is shown in grey. The holes in the t -sphere get patched with flat pieces. Relative sizes, shapes, and positions are not accurate.

categorization, we can write ϕ as

$$\phi = \begin{cases} \log \left| \frac{dz}{dt} \right|^2; & \text{regular region} \\ \log \left| \frac{d\tilde{z}}{dt} \right|^2; & \text{annuli} \\ \log \left| \frac{d\tilde{z}}{dt} \right|^2; & \text{second half of the } t\text{-sphere} \\ (\text{constant}); & \text{flat patches} \end{cases} \quad (\text{A.4})$$

Note that ϕ is a continuous function over Σ , but its first derivative is discontinuous across the boundaries between the above regions.

The goal of this appendix is to compute the Liouville action,

$$S_L = \frac{c}{96\pi} \int_{\tilde{\Sigma}} d^2t \sqrt{\hat{g}} \left[\partial_\mu \phi \partial_\nu \phi \hat{g}^{\mu\nu} + 2\hat{R}\phi \right], \quad (\text{A.5})$$

in the limit of small ε , $\tilde{\varepsilon}$, δ , and δ' . Any regularization dependence drops out once we normalize the twist operators to have unit two-point function with themselves at unit separation. It is important to note that the curvature and metric in the above equation are on the fiducial manifold $\tilde{\Sigma}$, and not the more complicated curved manifold Σ . This means, for instance, the only curvature contribution comes from the ring of concentrated curvature at $|t| = 1/\delta'$ where the two discs of the fiducial metric are glued together.

There are the following nonzero contributions to the Liouville action:

1. a contribution $S_L^{(1)}$ from the regular region R (light gray in the Figure 6).
2. a contribution $S_L^{(2)}$ from the annulus A , between the outer image of $|z| = \frac{1}{\delta}$ and $|t| = 1/\delta'$.
3. a contribution $S_L^{(3)}$ from the ring of curvature concentrated at $|t| = 1/\delta'$.
4. a contribution $S_L^{(4)}$ from the second half of the t -sphere, but outside of the patched hole around $\tilde{t} = 0$.
5. a contribution $S_L^{(5)}$ from the annuli around the finite images of infinity between the image of $|\tilde{z}| = \tilde{\varepsilon}$ and the image of $|z| = |\tilde{z}| = 1/\delta$.

The flat patches (and the various boundaries between the regions) do not contribute. In the flat regions, there is no curvature of the fiducial metric and ϕ is constant; therefore, there can be no contribution. On their boundaries, $\partial\phi$ is nonzero, but bounded and is integrated over a set of measure zero. Therefore, the edges of the filled holes do not contribute either. There can be no curvature contribution beyond $S_L^{(3)}$, but one may worry about possible kinetic term contributions from various boundaries; however, these cannot contribute as long as $\partial\phi$ is bounded, which means that as long as ϕ is continuous, there is no contribution from the kinetic term on boundaries. Note that the fourth and fifth contributions are zero for the calculations performed in [46].

A.1. The $S_L^{(1)}$ contributions

The regularization-independent contributions all come from the regular region, whose contribution is called $S_L^{(1)}$. We have

$$S_L^{(1)} = \frac{c}{96\pi} \int_{\Sigma_R} d^2t \sqrt{\hat{g}} [\partial_\mu \phi \partial_\nu \phi \hat{g}^{\mu\nu} + 2\hat{R}\phi], \quad (\text{A.6})$$

where the hats denote quantities computed with the fiducial metric

$$\hat{ds}^2 = dt d\bar{t} \quad |t| < \frac{1}{\delta'}. \quad (\text{A.7})$$

From Equation (A.4), one sees that in the regular region,

$$\phi = \log \frac{dz}{dt} + \log \frac{d\bar{z}}{d\bar{t}}. \quad (\text{A.8})$$

The fiducial metric has no curvature in the regular region Σ_R , and therefore

$$S_L^{(1)} = \frac{c}{96\pi} \int_{\Sigma_R} d^2t \partial_\mu \phi \partial^\mu \phi, \quad (\text{A.9})$$

which we can integrate by parts into

$$S_L^{(1)} = -\frac{c}{96\pi} \int_{\Sigma_R} d^2t \phi \partial_\mu \partial^\mu \phi + \frac{c}{96\pi} \int_{\partial\Sigma_R} \phi \partial_n \phi ds \quad (\text{A.10})$$

Since ϕ is the sum of a holomorphic part and an antiholomorphic part,

$$\partial_\mu \partial^\mu \phi = 4\partial\bar{\partial}\phi = 0, \quad (\text{A.11})$$

and therefore, we have only the boundary term to contend with. More explicitly, one may write

$$S_L^{(1)} = \frac{c}{96\pi} \left[i \int_{\partial\Sigma_R} dt \phi \partial\phi + \text{c.c.} \right]. \quad (\text{A.12})$$

Note that this equation assumes a convention where “internal” boundaries are integrated counter-clockwise and the “external” boundary is integrated clockwise. Alternatively, one may think of this prescription as integrating every contour counter-clockwise from the local perspective of someone living inside the hole (outside the region Σ_R) on the Riemann sphere. This means that the “external” hole should be viewed from ∞ /North pole of the Riemann sphere, which switches the contour’s orientation from the perspective of someone living in the finite t plane.

The boundary of Σ_R is composed of

1. the hole around the origin from the twist of order $\kappa(l+1)$.
2. the hole around $t=1$ from the twist of order $(l+1)$ at z_2 .
3. the l images of $|z|=1/\delta$ in the finite t plane.
4. the outer boundary from the image of $|z|=1/\delta$.

Note that each of the $(l+1)$ images of infinity corresponds to one of the $(l+1)$ σ_κ twists inserted at infinity. All contours should be counter-clockwise, except for the contour circling $t \rightarrow \infty$.

We begin by finding the contribution from the hole around the origin. We make this calculation most explicit. Near the origin

$$z \approx (-1)^{\kappa l} z_2 t^{\kappa(l+1)} \quad \frac{dz}{dt} \approx (-1)^{\kappa l} \kappa(l+1) z_2 t^{\kappa(l+1)-1},$$

and therefore (from here on we implicitly work in the limit of small $\varepsilon, \tilde{\varepsilon}, \delta, \delta'$ and drop approximation signs)

$$\begin{aligned} \phi &= 2 \log(\kappa(l+1)) + 2 \log|z_2| + 2[\kappa(l+1) - 1] \log|t| \\ \partial\phi &= \frac{\kappa(l+1) - 1}{t}. \end{aligned} \quad (\text{A.13})$$

Since the hole is of size ε in the z -plane, the contour in the t -space should have

$$|t| = \left(\frac{\varepsilon}{|z_2|} \right)^{\frac{1}{\kappa(l+1)}}. \quad (\text{A.14})$$

Therefore, we parameterize the contour as

$$t = \left(\frac{\varepsilon}{|z_2|} \right)^{\frac{1}{\kappa(l+1)}} e^{i\theta} \quad dt = it d\theta. \quad (\text{A.15})$$

Thus,

$$\begin{aligned}
S_L^{(1)}(t=0) &= \frac{c}{96\pi} \left\{ -2[\kappa(l+1)-1] \int_0^{2\pi} d\theta \left[\log(\kappa(l+1)) + \log|z_2| + \frac{\kappa(l+1)-1}{\kappa(l+1)} \log \frac{\varepsilon}{|z_2|} \right] \right\} \\
&\quad + \text{c.c} \\
&= -\frac{c}{12} (\kappa(l+1)-1) \left[\frac{1}{\kappa(l+1)} \log|z_2| + \log \kappa(l+1) + \frac{\kappa(l+1)-1}{\kappa(l+1)} \log \varepsilon \right]. \quad (\text{A.16})
\end{aligned}$$

For $t=1$, since

$$z \approx z_2 + z_2 \kappa (t-1)^{l+1} \quad \frac{dz}{dt} \approx z_2 \kappa (l+1) (t-1)^l,$$

we have

$$\begin{aligned}
\phi &= 2 \log|z_2| + 2 \log \kappa(l+1) + 2l \log|t-1| \\
\partial\phi &= \frac{l}{t-1} \\
t &= 1 + \left(\frac{\varepsilon}{\kappa|z_2|} \right)^{\frac{1}{l+1}} e^{i\theta} \quad dt = i(t-1)d\theta. \quad (\text{A.17})
\end{aligned}$$

Plugging in, one finds

$$S_L^{(1)}(t=1) = -\frac{c}{12} l \left[\frac{1}{l+1} \log|z_2| + \frac{1}{l+1} \log(\kappa(l+1)^{l+1}) + \frac{l}{l+1} \log \varepsilon \right]. \quad (\text{A.18})$$

The only difference for $t=\infty$ is that the contour is clockwise which gives an extra minus sign. From above, we know that

$$z \approx \frac{z_2}{(l+1)^\kappa} t^\kappa \quad \frac{dz}{dt} \approx \frac{z_2 \kappa}{(l+1)^\kappa} t^{\kappa-1},$$

and therefore

$$\begin{aligned}
\phi &= 2 \log|z_2| + 2 \log \frac{\kappa}{(l+1)^\kappa} + 2(\kappa-1) \log|t| \\
\partial\phi &= \frac{\kappa-1}{t} \\
t &= \frac{l+1}{(\delta|z_2|)^{\frac{1}{\kappa}}} e^{-i\theta} \quad dt = -itd\theta. \quad (\text{A.19})
\end{aligned}$$

Thus,

$$S_L^{(1)}(t \rightarrow \infty) = \frac{c}{12} (\kappa-1) \left[\frac{1}{\kappa} \log|z_2| + \log \frac{\kappa}{l+1} - \frac{\kappa-1}{\kappa} \log \delta \right]. \quad (\text{A.20})$$

Finally, the only other contribution to $S_L^{(1)}$ comes from the images of $z \rightarrow \infty$ that are in the finite t -plane. Near one of the $t_\infty^{(j)}$,⁵

$$z \approx z_2 \left[\frac{\alpha_j}{(l+1)(1-\alpha_j)^2} \right]^\kappa \frac{1}{(t-t_\infty^{(j)})^\kappa} \quad \frac{dz}{dt} \approx -\kappa z_2 \left[\frac{\alpha_j}{(l+1)(1-\alpha_j)^2} \right]^\kappa \frac{1}{(t-t_\infty^{(j)})^{\kappa+1}},$$

⁵ we dropped some irrelevant minus signs in the map.

where recall that the

$$t_\infty^{(j)} = \frac{1}{1 - \alpha_j}.$$

For convenience, we define

$$\beta_j = \left[\frac{\alpha_j}{(l+1)(1-\alpha_j)^2} \right]^\kappa = \frac{1}{[(l+1)\alpha_j^l(1-\alpha_j)^2]^\kappa}. \quad (\text{A.21})$$

The above yields

$$\begin{aligned} \phi &= 2 \log |z_2| + 2 \log \kappa |\beta_j| - 2(\kappa + 1) \log |t - t_\infty^{(j)}| \\ \partial \phi &= -\frac{\kappa + 1}{t - t_\infty^{(j)}} \\ t &= t_\infty^{(j)} + (|z_2| |\beta_j| \delta)^{\frac{1}{\kappa}} e^{i\theta} \quad dt = i(t - t_\infty^{(j)}) d\theta. \end{aligned} \quad (\text{A.22})$$

Being careful of minus signs, one finds

$$S_L^{(1)}(t = t_\infty^{(j)}) = -\frac{c}{12}(\kappa + 1) \left[\frac{1}{\kappa} \log |z_2| - \log \kappa + \frac{1}{\kappa} \log |\beta_j| + \frac{\kappa + 1}{\kappa} \log \delta \right]. \quad (\text{A.23})$$

Adding all l contributions from finite images of infinity,

$$\sum_{j=1}^l S_L^{(1)}(t_\infty^{(j)}) = -\frac{c}{12}(\kappa + 1)l \left[\frac{1}{\kappa} \log |z_2| - \log \kappa + \frac{\kappa + 1}{\kappa} \log \delta \right] - \frac{c}{12} \frac{\kappa + 1}{\kappa} \sum_{j=1}^l \log |\beta_j|. \quad (\text{A.24})$$

To simplify the final term note that

$$\sum_{j=1}^l \log |\beta_j| = -\kappa \sum_{j=1}^l \log \left[(l+1) |\alpha_j^l (1 - \alpha_j)^2| \right] = -\kappa l \log(l+1) - \kappa \log \left| \prod_{j=1}^l \alpha_j^l (1 - \alpha_j)^2 \right|. \quad (\text{A.25})$$

Thus, we become interested in computing

$$\begin{aligned} \prod_{j=1}^l \alpha_j^l (1 - \alpha_j)^2 &= \frac{\left(\prod_{j=1}^l (1 - \alpha_j) \right)^2}{\prod_{j=1}^l \alpha_j} \\ &= (l+1)^2, \end{aligned} \quad (\text{A.26})$$

where we have used (from [46] Equation (3.16))⁶

$$\prod_{j=1}^l \alpha_j = (-1)^l \quad \prod_{j=1}^l (q - \alpha_j) = \frac{q^{l+1} - 1}{q - 1} \xrightarrow{q \rightarrow 1} l + 1. \quad (\text{A.27})$$

Therefore, the total contribution from the finite images of infinity is

$$\begin{aligned} \sum_{j=1}^l S_L^{(1)}(t_\infty^{(j)}) &= -\frac{c}{12}(\kappa + 1)l \left[\frac{1}{\kappa} \log |z_2| - \log \kappa + \frac{\kappa + 1}{\kappa} \log \delta \right] + \frac{c}{12}(\kappa + 1)(l + 2) \log(l + 1) \\ &= -\frac{c}{12}(\kappa + 1)l \left[\frac{1}{\kappa} \log |z_2| - \log \kappa - \frac{l + 2}{l} \log(l + 1) + \frac{\kappa + 1}{\kappa} \log \delta \right]. \end{aligned} \quad (\text{A.28})$$

⁶ There is an error in [46], which does not affect the final answer.

Summing up all of the contributions, we find that

$$\begin{aligned}
S_L^{(1)} = -\frac{c}{12} & \left\{ \frac{(\kappa+1)l(l+2)}{\kappa(l+1)} \log |z_2| \right. \\
& - \frac{l^2}{l+1} \log \kappa \\
& - 4 \log(l+1) \\
& + \frac{1}{l+1} \left(l^2(\kappa+1) + 2l(\kappa-1) + \frac{(\kappa-1)^2}{\kappa} \right) \log \varepsilon \\
& \left. + \left(\frac{l+1}{\kappa}(\kappa^2+1) + 2(l-1) \right) \log \delta \right\}.
\end{aligned} \tag{A.29}$$

Let's examine the z_2 dependence. The expected power of $|z_2|$ for the correlator is

$$\begin{aligned}
-2(\Delta_{\kappa(l+1)} + \Delta_{l+1} - (l+1)\Delta_\kappa) &= -\frac{c}{12} \left[\kappa(l+1) - \frac{1}{\kappa(l+1)} + (l+1) - \frac{1}{l+1} \right. \\
& \quad \left. - (l+1) \left(\kappa - \frac{1}{\kappa} \right) \right] \\
&= -\frac{c}{12} \frac{(\kappa+1)l(l+2)}{\kappa(l+1)}.
\end{aligned} \tag{A.30}$$

This exactly matches the contribution from $S_L^{(1)}$. Therefore, any other contributions' $|z_2|$ -dependence should cancel out.

A.2. The contribution $S_L^{(2)}$

We now compute the contribution to the Liouville action from the outer annulus between the image of $|z| = 1/\delta$ and $|t| = 1/\delta'$. From the behavior of the map for large t ,

$$z \approx \frac{z_2}{(l+1)^\kappa} t^\kappa$$

we see that the region for this contribution is defined by

$$\frac{l+1}{(|z_2|\delta)^{\frac{1}{\kappa}}} < |t| < \frac{1}{\delta'}. \tag{A.31}$$

The induced metric for this region comes from the second half of the z -plane:

$$ds^2 = d\tilde{z}d\bar{\tilde{z}} = \frac{d\tilde{z}}{dt} \frac{d\bar{\tilde{z}}}{d\bar{t}} dt d\bar{t} = e^\phi dt d\bar{t}. \tag{A.32}$$

Thus, we should look at

$$\begin{aligned}
\tilde{z} &= \frac{1}{\delta^2} \frac{(l+1)^\kappa}{z_2 t^\kappa} & \frac{d\tilde{z}}{dt} &= -\frac{\kappa}{\delta^2} \frac{(l+1)^\kappa}{z_2 t^{\kappa+1}} \\
\phi &= 2[\log \kappa(l+1)^\kappa - 2 \log \delta - \log |z_2| - (\kappa+1) \log |t|] \\
\partial\phi &= -\frac{\kappa+1}{t}.
\end{aligned} \tag{A.33}$$

One can integrate by parts, or integrate directly, as we do below:

$$\begin{aligned}
S_L^{(2)} &= \frac{4c}{96\pi} \int d^2t \partial\phi \bar{\partial}\phi \\
&= \frac{c}{24\pi} \int (2\pi|t|d|t|) \frac{(\kappa+1)^2}{|t|^2} \\
&= \frac{c}{12} (\kappa+1)^2 \int \frac{d|t|}{|t|} \\
&= \frac{c}{12} \frac{(\kappa+1)^2}{\kappa} \log \frac{|z_2|\delta}{((l+1)\delta')^\kappa}.
\end{aligned} \tag{A.34}$$

A.3. The contribution $S_L^{(3)}$

Here we are just concerned with the curvature term. Since all of the curvature is concentrated along the ring $|t| = 1/\delta'$, we find

$$S_L^{(3)} = \frac{c}{48\pi} \int d^2t \hat{R}\phi = \frac{c}{6} \phi|_{|t|=1/\delta'}. \tag{A.35}$$

From above, we see that

$$\begin{aligned}
\phi &= 2 \left[\log \kappa(l+1)^\kappa - 2 \log \delta - \log |z_2| - (\kappa+1) \log |t| \right] \\
&= -2 \left[\log |z_2| - \log \kappa(l+1)^\kappa + \log \frac{\delta^2}{\delta'^{\kappa+1}} \right].
\end{aligned} \tag{A.36}$$

Plugging in, one finds

$$S_L^{(3)} = -\frac{c}{3} \left[\log |z_2| - \log \kappa(l+1)^\kappa + \log \frac{\delta^2}{\delta'^{\kappa+1}} \right]. \tag{A.37}$$

A.4. The contribution $S_L^{(4)}$

We now calculate our first new contribution. We should find that it vanishes for $\kappa = 1$. The map in this region is between \tilde{z} and \tilde{t} :

$$\begin{aligned}
\tilde{z} &= \left(\frac{\delta'^\kappa}{\delta} \right)^2 \frac{(l+1)^\kappa}{z_2} \tilde{t}^\kappa & \frac{d\tilde{z}}{d\tilde{t}} &= \left(\frac{\delta'^\kappa}{\delta} \right)^2 \frac{\kappa(l+1)^\kappa}{z_2} \tilde{t}^{\kappa-1} \\
\phi &= 2 \left[\log \kappa(l+1)^\kappa - \log |z_2| + 2 \log \frac{\delta'^\kappa}{\delta} + (\kappa-1) \log |\tilde{t}| \right] \\
\partial\phi &= \frac{\kappa-1}{\tilde{t}}.
\end{aligned} \tag{A.38}$$

As for $S_L^{(2)}$, it may be more convenient to integrate directly over the region,

$$\frac{1}{l+1} \left(\tilde{\varepsilon} \frac{\delta^2}{\delta'^{2\kappa}} |z_2| \right)^{\frac{1}{\kappa}} < |\tilde{t}| < \frac{1}{\delta'}. \tag{A.39}$$

Proceeding, one finds

$$\begin{aligned} S_L^{(4)} &= \frac{c}{12} (\kappa - 1)^2 \int \frac{d|t|}{|t|} \\ &= \frac{c}{12} \frac{(\kappa - 1)^2}{\kappa} \log \frac{(l + 1)^\kappa \delta'^\kappa}{|z_2| \tilde{\varepsilon} \delta^2}. \end{aligned} \quad (\text{A.40})$$

A.5. The contribution $S_L^{(5)}$

Finally, all that remains is the contribution from the annuli surrounding the finite images of infinity, where the induced metric comes from the second half of the z -sphere. Hence, the map is between \tilde{z} and t :

$$z = z_2 \beta_j \frac{1}{(t - t_\infty^{(j)})^\kappa} \implies \tilde{z} = \frac{1}{\delta^2} \frac{(t - t_\infty)^\kappa}{z_2 \beta}, \quad (\text{A.41})$$

where we have given the map near the j th finite image of infinity. Note that we dropped the index j , since it can be shown that all of the annuli give the same contribution.

The region, of interest is

$$(\delta^2 \tilde{\varepsilon} |z_2| |\beta|)^{\frac{1}{\kappa}} < |t - t_\infty| < (\delta |z_2| |\beta|)^{\frac{1}{\kappa}}. \quad (\text{A.42})$$

Once again, we find it most convenient to integrate directly, in which case, we need only know

$$\partial \phi = \frac{\kappa - 1}{t - t_\infty}. \quad (\text{A.43})$$

Integrating, one produces the expression for the contribution from *one* of the annuli:

$$S_L^{(5)}(t_\infty^{(j)}) = -\frac{c}{12} \frac{(\kappa - 1)^2}{\kappa} \log(\tilde{\varepsilon} \delta). \quad (\text{A.44})$$

As claimed, the contribution did not depend on which finite image of infinity under consideration; therefore, one computes the total contribution of this kind by multiplying the above expression by l to find

$$S_L^{(5)} = -\frac{c}{12} \frac{l(\kappa - 1)^2}{\kappa} \log(\tilde{\varepsilon} \delta). \quad (\text{A.45})$$

A.6. Adding up all of the contributions

For convenience, we collect all of the contributions:

$$\begin{aligned} S_L^{(1)} &= -\frac{c}{12} \left\{ \frac{(\kappa + 1)l(l + 2)}{\kappa(l + 1)} \log |z_2| \right. \\ &\quad - \frac{l^2}{l + 1} \log \kappa \\ &\quad - 4 \log(l + 1) \\ &\quad + \frac{1}{l + 1} \left(l^2(\kappa + 1) + 2l(\kappa - 1) + \frac{(\kappa - 1)^2}{\kappa} \right) \log \varepsilon \\ &\quad \left. + \left(\frac{l + 1}{\kappa} (\kappa^2 + 1) + 2(l - 1) \right) \log \delta \right\} \end{aligned} \quad (\text{A.46a})$$

$$S_L^{(2)} = \frac{c}{12} \frac{(\kappa+1)^2}{\kappa} \log \frac{|z_2| \delta}{((l+1)\delta')^\kappa} \quad (\text{A.46b})$$

$$S_L^{(3)} = -\frac{c}{3} \left[\log |z_2| - \log \kappa (l+1)^\kappa + \log \frac{\delta^2}{\delta'^{\kappa+1}} \right] \quad (\text{A.46c})$$

$$S_L^{(4)} = \frac{c}{12} \frac{(\kappa-1)^2}{\kappa} \log \frac{(l+1)^\kappa \delta'^\kappa}{|z_2| \tilde{\varepsilon} \delta^2} \quad (\text{A.46d})$$

$$S_L^{(5)} = -\frac{c}{12} \frac{l(\kappa-1)^2}{\kappa} \log(\tilde{\varepsilon} \delta). \quad (\text{A.46e})$$

Note that the $|z_2|$ dependence of $S_L^{(2)}$ through $S_L^{(5)}$ cancels out, leaving us, correctly, with just the dependence of $S_L^{(1)}$. Another check is to compute the δ' dependence,

$$\delta' : \quad \frac{c}{3} \log \delta', \quad (\text{A.47a})$$

which is exactly the correct dependence to get cancelled by $Z_{\delta'}$ in Equation (6.13). We discuss this in more detail in Section 6.3. Computing the $\tilde{\varepsilon}$ dependence, one finds

$$\tilde{\varepsilon} : \quad -\frac{c}{12} \frac{(l+1)(\kappa-1)^2}{\kappa} \log \tilde{\varepsilon}, \quad (\text{A.47b})$$

which should get canceled out by the normalization of the two-point function. The δ dependence is a bit more tedious to work out, but comes to

$$\delta : \quad -\frac{c}{12} \frac{2(l+1)(\kappa^2+1)}{\kappa} \log \delta. \quad (\text{A.47c})$$

Finally, there is the regularization-independent part, about which we cannot say anything until we normalize the twists in Section 6.3:

$$\begin{aligned} \kappa : \quad & \frac{c}{12} \frac{(l+2)^2}{l+1} \log \kappa \\ (l+1) : \quad & \frac{c}{3} \log(l+1). \end{aligned} \quad (\text{A.47d})$$

Putting all of the pieces together, we have the expression for the total Liouville action:

$$\begin{aligned} S_L^{\text{tot.}} = -\frac{c}{12} \Big\{ & \frac{(\kappa+1)l(l+2)}{\kappa(l+1)} \log |z_2| \\ & - \frac{(l+2)^2}{l+1} \log \kappa - 4 \log(l+1) \\ & + \frac{1}{l+1} \left(l^2(\kappa+1) + 2l(\kappa-1) + \frac{(\kappa-1)^2}{\kappa} \right) \log \varepsilon \\ & + \frac{(l+1)(\kappa-1)^2}{\kappa} \log \tilde{\varepsilon} \\ & + \frac{2(l+1)(\kappa^2+1)}{\kappa} \log \delta \\ & - 4 \log \delta' \Big\}. \end{aligned} \quad (\text{A.48})$$

APPENDIX B: THE TWO-POINT FUNCTION FOR TWISTS AT INFINITY

In order to normalize the correlator, we need to compute the two-point function of σ_κ at the origin with σ_κ at infinity using the same regularizations as in Appendix A. The map is simply

$$z = bt^\kappa. \quad (\text{B.1})$$

To find the total Liouville action for this map, we recognize that this case is given by setting $l = 0$ in the calculation of Appendix A:

$$S_L^{\text{tot.}} = -\frac{c}{12} \left\{ -4 \log \kappa + \frac{(\kappa-1)^2}{\kappa} \log \varepsilon + \frac{(\kappa-1)^2}{\kappa} \log \tilde{\varepsilon} + 2 \frac{\kappa^2+1}{\kappa} \log \delta - 4 \log \delta' \right\}. \quad (\text{B.2})$$

Note that the b dependence cancelled out, as it must.

Since the two-point correlator is given by

$$\langle \sigma_\kappa(\infty) \sigma_\kappa(0) \rangle = e^{S_L} \frac{Z_{\delta'}}{(Z_\delta)^\kappa},$$

and

$$Z_\delta = Q \delta^{-\frac{c}{3}} \quad Z_{\delta'} = Q \delta'^{-\frac{c}{3}}, \quad (\text{B.3})$$

the two-point function is given by

$$\langle \sigma_\kappa(\infty)^{\tilde{\varepsilon}, \delta} \sigma_\kappa(0)^\varepsilon \rangle_\delta = \frac{\kappa^{\frac{c}{3}} \delta^{\frac{c}{6} \frac{\kappa^2-1}{\kappa}}}{Q^{\kappa-1} (\varepsilon \tilde{\varepsilon})^{\frac{1}{12} \frac{(\kappa-1)^2}{\kappa}}}. \quad (\text{B.4})$$

Note that if we attempted to normalize the two twists using Equation (6.32) (with respect to their local appearance), then one finds the correlator of the normalized twists is

$$\langle \sigma_\kappa(\infty) \sigma_\kappa(0) \rangle_\delta = \delta^{\frac{c}{6} \frac{\kappa^2-1}{\kappa}} = \delta^{4\Delta_\kappa}, \quad (\text{B.5})$$

exactly what one would expect for the two-point function of two normalized twists with one at the origin and one at $|z| = 1/\delta$.

-
- [1] S. G. Avery, B. D. Chowdhury, and S. D. Mathur, “Emission from the D1D5 CFT”, 0906.2015.
 - [2] V. Jejjala, O. Madden, S. F. Ross, and G. Titchener, “Non-supersymmetric smooth geometries and D1-D5-P bound states”, *Phys. Rev.* **D71** (2005) 124030, hep-th/0504181.
 - [3] V. Balasubramanian, J. de Boer, S. El-Showk, and I. Messamah, “Black Holes as Effective Geometries”, *Class. Quant. Grav.* **25** (2008) 214004, 0811.0263.
 - [4] O. Lunin and S. D. Mathur, “AdS/CFT duality and the black hole information paradox”, *Nucl. Phys.* **B623** (2002) 342–394, hep-th/0109154.
 - [5] O. Lunin and S. D. Mathur, “Statistical interpretation of Bekenstein entropy for systems with a stretched horizon”, *Phys. Rev. Lett.* **88** (2002) 211303, hep-th/0202072.
 - [6] O. Lunin, J. M. Maldacena, and L. Maoz, “Gravity solutions for the D1-D5 system with angular momentum”, hep-th/0212210.
 - [7] S. D. Mathur, A. Saxena, and Y. K. Srivastava, “Constructing ‘hair’ for the three charge hole”, *Nucl. Phys.* **B680** (2004) 415–449, hep-th/0311092.
 - [8] S. Giusto, S. D. Mathur, and A. Saxena, “Dual geometries for a set of 3-charge microstates”, *Nucl. Phys.* **B701** (2004) 357–379, hep-th/0405017.

- [9] S. Giusto, S. D. Mathur, and A. Saxena, “3-charge geometries and their CFT duals”, *Nucl. Phys.* **B710** (2005) 425–463, hep-th/0406103.
- [10] M. Taylor, “General 2 charge geometries”, *JHEP* **03** (2006) 009, hep-th/0507223.
- [11] I. Kanitscheider, K. Skenderis, and M. Taylor, “Fuzzballs with internal excitations”, *JHEP* **06** (2007) 056, 0704.0690.
- [12] K. Skenderis and M. Taylor, “Fuzzball solutions and D1-D5 microstates”, *Phys. Rev. Lett.* **98** (2007) 071601, hep-th/0609154.
- [13] I. Kanitscheider, K. Skenderis, and M. Taylor, “Holographic anatomy of fuzzballs”, *JHEP* **04** (2007) 023, hep-th/0611171.
- [14] I. Bena, C.-W. Wang, and N. P. Warner, “Plumbing the Abyss: Black Ring Microstates”, *JHEP* **07** (2008) 019, 0706.3786.
- [15] I. Bena, N. Bobev, and N. P. Warner, “Spectral Flow, and the Spectrum of Multi-Center Solutions”, *Phys. Rev.* **D77** (2008) 125025, 0803.1203.
- [16] I. Bena, N. Bobev, C. Ruef, and N. P. Warner, “Entropy Enhancement and Black Hole Microstates”, 0804.4487.
- [17] I. Bena, N. Bobev, C. Ruef, and N. P. Warner, “Supertubes in Bubbling Backgrounds: Born-Infeld Meets Supergravity”, 0812.2942.
- [18] P. Berglund, E. G. Gimon, and T. S. Levi, “Supergravity microstates for BPS black holes and black rings”, *JHEP* **06** (2006) 007, hep-th/0505167.
- [19] V. Balasubramanian, E. G. Gimon, and T. S. Levi, “Four Dimensional Black Hole Microstates: From D-branes to Spacetime Foam”, *JHEP* **01** (2008) 056, hep-th/0606118.
- [20] E. G. Gimon and T. S. Levi, “Black Ring Deconstruction”, *JHEP* **04** (2008) 098, 0706.3394.
- [21] E. G. Gimon, T. S. Levi, and S. F. Ross, “Geometry of non-supersymmetric three-charge bound states”, *JHEP* **08** (2007) 055, 0705.1238.
- [22] J. de Boer, F. Denef, S. El-Showk, I. Messamah, and D. Van den Bleeken, “Black hole bound states in $AdS_3 \times S^2$ ”, *JHEP* **11** (2008) 050, 0802.2257.
- [23] J. de Boer, S. El-Showk, I. Messamah, and D. V. d. Bleeken, “Quantizing N=2 Multicenter Solutions”, 0807.4556.
- [24] S. D. Mathur, “The fuzzball proposal for black holes: An elementary review”, *Fortsch. Phys.* **53** (2005) 793–827, hep-th/0502050.
- [25] S. D. Mathur, “The quantum structure of black holes”, *Class. Quant. Grav.* **23** (2006) R115, hep-th/0510180.
- [26] I. Bena and N. P. Warner, “Black holes, black rings and their microstates”, *Lect. Notes Phys.* **755** (2008) 1–92, hep-th/0701216.
- [27] K. Skenderis and M. Taylor, “The fuzzball proposal for black holes”, *Phys. Rept.* **467** (2008) 117–171, 0804.0552.
- [28] A. Saxena, G. Potvin, S. Giusto, and A. W. Peet, “Smooth geometries with four charges in four dimensions”, *JHEP* **04** (2006) 010, hep-th/0509214.
- [29] J. Ford, S. Giusto, and A. Saxena, “A class of BPS time-dependent 3-charge microstates from spectral flow”, *Nucl. Phys.* **B790** (2008) 258–280, hep-th/0612227.
- [30] S. Giusto and A. Saxena, “Stationary axisymmetric solutions of five dimensional gravity”, *Class. Quant. Grav.* **24** (2007) 4269–4294, 0705.4484.
- [31] J. Ford, S. Giusto, A. Peet, and A. Saxena, “Reduction without reduction: Adding KK-monopoles to five dimensional stationary axisymmetric solutions”, *Class. Quant. Grav.* **25** (2008) 075014, 0708.3823.
- [32] S. Giusto, S. F. Ross, and A. Saxena, “Non-supersymmetric microstates of the D1-D5-KK system”, *JHEP* **12** (2007) 065, 0708.3845.
- [33] S. S. Gubser, I. R. Klebanov, and A. M. Polyakov, “Gauge theory correlators from non-critical string theory”, *Phys. Lett.* **B428** (1998) 105–114, hep-th/9802109.
- [34] E. Witten, “Anti-de Sitter space and holography”, *Adv. Theor. Math. Phys.* **2** (1998) 253–291, hep-th/9802150.
- [35] O. Aharony, S. S. Gubser, J. M. Maldacena, H. Ooguri, and Y. Oz, “Large N field theories, string theory and gravity”, *Phys. Rept.* **323** (2000) 183–386, hep-th/9905111.
- [36] B. D. Chowdhury and S. D. Mathur, “Non-extremal fuzzballs and ergoregion emission”, *Class. Quant. Grav.* **26** (2009) 035006, 0810.2951.

- [37] J. M. Maldacena, “The large N limit of superconformal field theories and supergravity”, *Adv. Theor. Math. Phys.* **2** (1998) 231–252, hep-th/9711200.
- [38] N. Seiberg and E. Witten, “The D1/D5 system and singular CFT”, *JHEP* **04** (1999) 017, hep-th/9903224.
- [39] F. Larsen and E. J. Martinec, “U(1) charges and moduli in the D1-D5 system”, *JHEP* **06** (1999) 019, hep-th/9905064.
- [40] J. de Boer, “Six-dimensional supergravity on $S^3 \times \text{AdS}(3)$ and 2d conformal field theory”, *Nucl. Phys.* **B548** (1999) 139–166, hep-th/9806104.
- [41] R. Dijkgraaf, “Instanton strings and hyperKähler geometry”, *Nucl. Phys.* **B543** (1999) 545–571, hep-th/9810210.
- [42] G. E. Arutyunov and S. A. Frolov, “Virasoro amplitude from the $S(N)$ R^{24} orbifold sigma model”, *Theor. Math. Phys.* **114** (1998) 43–66, hep-th/9708129.
- [43] G. E. Arutyunov and S. A. Frolov, “Four graviton scattering amplitude from $S(N)$ R^8 supersymmetric orbifold sigma model”, *Nucl. Phys.* **B524** (1998) 159–206, hep-th/9712061.
- [44] A. Jevicki, M. Mihailescu, and S. Ramgoolam, “Gravity from CFT on $S^N(X)$: Symmetries and interactions”, *Nucl. Phys.* **B577** (2000) 47–72, hep-th/9907144.
- [45] J. R. David, G. Mandal, S. Vaidya, and S. R. Wadia, “Point mass geometries, spectral flow and $\text{AdS}(3)$ -CFT(2) correspondence”, *Nucl. Phys.* **B564** (2000) 128–141, hep-th/9906112.
- [46] O. Lunin and S. D. Mathur, “Correlation functions for $M(N)/S(N)$ orbifolds”, *Commun. Math. Phys.* **219** (2001) 399–442, hep-th/0006196.
- [47] V. Cardoso, O. J. C. Dias, J. L. Hovdebo, and R. C. Myers, “Instability of non-supersymmetric smooth geometries”, *Phys. Rev.* **D73** (2006) 064031, hep-th/0512277.
- [48] B. D. Chowdhury and S. D. Mathur, “Radiation from the non-extremal fuzzball”, *Class. Quant. Grav.* **25** (2008) 135005, 0711.4817.
- [49] B. D. Chowdhury and S. D. Mathur, “Pair creation in non-extremal fuzzball geometries”, *Class. Quant. Grav.* **25** (2008) 225021, 0806.2309.
- [50] J. M. Maldacena and L. Maoz, “De-singularization by rotation”, *JHEP* **12** (2002) 055, hep-th/0012025.
- [51] V. Balasubramanian, J. de Boer, E. Keski-Vakkuri, and S. F. Ross, “Supersymmetric conical defects: Towards a string theoretic description of black hole formation”, *Phys. Rev.* **D64** (2001) 064011, hep-th/0011217.
- [52] A. Schwimmer and N. Seiberg, “Comments on the $N=2$, $N=3$, $N=4$ Superconformal Algebras in Two-Dimensions”, *Phys. Lett.* **B184** (1987) 191.
- [53] O. Lunin and S. D. Mathur, “Three-point functions for $M(N)/S(N)$ orbifolds with $N = 4$ supersymmetry”, *Commun. Math. Phys.* **227** (2002) 385–419, hep-th/0103169.
- [54] M. Yu, “THE UNITARY REPRESENTATIONS OF THE $N=4$ $SU(2)$ EXTENDED SUPERCONFORMAL ALGEBRAS”, *Nucl. Phys.* **B294** (1987) 890.
- [55] W. Lerche, C. Vafa, and N. P. Warner, “Chiral Rings in $N=2$ Superconformal Theories”, *Nucl. Phys.* **B324** (1989) 427.
- [56] A. Pakman, L. Rastelli, and S. S. Razamat, “Extremal Correlators and Hurwitz Numbers in Symmetric Product Orbifolds”, 0905.3451.
- [57] A. Pakman, L. Rastelli, and S. S. Razamat, “Diagrams for Symmetric Product Orbifolds”, 0905.3448.
- [58] D. Friedan, “INTRODUCTION TO POLYAKOV’S STRING THEORY”, To appear in Proc. of Summer School of Theoretical Physics: Recent Advances in Field Theory and Statistical Mechanics, Les Houches, France, Aug 2-Sep 10, 1982.
- [59] A. Strominger and C. Vafa, “Microscopic Origin of the Bekenstein-Hawking Entropy”, *Phys. Lett.* **B379** (1996) 99–104, hep-th/9601029.
- [60] C. G. Callan and J. M. Maldacena, “D-brane Approach to Black Hole Quantum Mechanics”, *Nucl. Phys.* **B472** (1996) 591–610, hep-th/9602043.
- [61] A. Dhar, G. Mandal, and S. R. Wadia, “Absorption vs decay of black holes in string theory and T-symmetry”, *Phys. Lett.* **B388** (1996) 51–59, hep-th/9605234.
- [62] S. R. Das and S. D. Mathur, “Comparing decay rates for black holes and D-branes”, *Nucl. Phys.* **B478** (1996) 561–576, hep-th/9606185.
- [63] S. R. Das and S. D. Mathur, “Interactions involving D-branes”, *Nucl. Phys.* **B482** (1996) 153–172,

- hep-th/9607149.
- [64] J. M. Maldacena and A. Strominger, “Black hole greybody factors and D-brane spectroscopy”, *Phys. Rev. D* **55** (1997) 861–870, hep-th/9609026.